5 Results

5.1 Generation and purification of an NS5A-specific antiserum.

5.1.1 Generation of an antiserum directed against the C-terminus of NS5A.

In order to work with NS5A at the protein level, it was essential to have a specific antiserum available. Since purification of full-length NS5A turned out to be quite difficult, an NS5A deletion mutant (NS5A (211-449)) was expressed by infection of Sf21 cells with a recombinant baculovirus. This deletion mutant encodes for the C-terminal half of NS5A (amino acids 211 to 449). It is expressed as a fusion protein with an N-terminal *Strep* tag and a C-terminal V5-epitope (Strep-NS5A(211-449)-V5). Sf21-derived Strep-NS5A(211-449)-V5 was purified by *Strep*Tactin Sepharose. Purified eluate fractions (E2 and E3) were subjected to SDS-PAGE and analyzed by silver staining or by Western blotting using a V5-specific antibody.

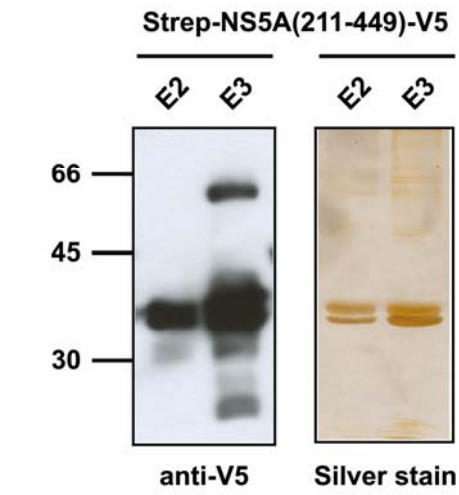

Fig. 5.1 Strep-NS5A(211-449)-V5 is purified by *Strep*Tactin Sepharose chromatography. Strep-NS5A(211-449)-V5 was expressed in Sf21 cells by the means of a recombinant baculovirus. Strep-NS5A(211-449)-V5 was purified by *Strep*Tactin Sepharose chromatography. Eluate fractions E2 and E3 were analyzed by Western blotting using a V5-specific antibody (Invitrogen) or by silver staining.

As illustrated in Fig. 5.1, Strep-NS5A(211-449)-V5 is produced in Sf21 cells. Purification by *Strep*Tactin Sepharose yields highly purified Strep-NS5A(211-449)-V5. Identity of the protein was confirmed by Western blotting using a V5-specific antibody.
This experiment indicates that NS5A(211-449) – unlike full-length NS5A – is expressed at high levels and readily accessible for purification by *Strep*Tactin Sepharose.
Eluate fractions containing NS5A(211-449) were pooled. One rabbit was immunized with the pooled eluate according to the protocol described in chapter 4.4.1. Two weeks after the final immunization, the rabbit was sacrificed and the serum was harvested by centrifugation of the peripheral blood.

5.1.2 Analysis of the NS5A-specific antiserum.

To analyze the specificity of the rabbit-derived antiserum, HuH-7 cells and HCV replicon cells HuH-7 I_{377}/NS3-3`/wt/9-13 were analyzed by immunofluorescence microscopy. As mentioned in chapter 1.7, these cells contain autonomously-replicating subgenomic HCV RNA and stably express the non-structural region of the HCV genome, so they contain high levels of NS5A.
HCV replicon cells were fixed and stained with the NS5A-specific antiserum. Naïve HuH-7 cells were included as a negative control. The background staining in HuH-7 cells was dimmed to darkness.

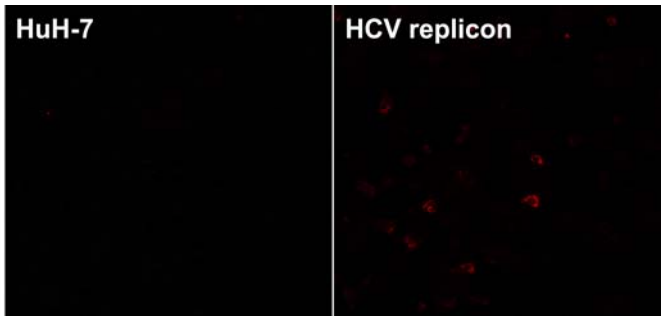

Fig. 5.2 The rabbit-derived antiserum recognizes NS5A in HCV replicon cells. HCV replicon cells HuH-7 I_{377}/NS3-3`/wt/9-13 or naïve HuH-7 cells were fixed in ethanol and stained with the NS5A-specific antiserum. NS5A was visualized using a Cy3-coupled secondary antibody. Samples were analyzed by confocal laser scanning microscopy (Magnification 100X).

Fig. 5.2 shows that the rabbit-derived antiserum detects a signal in HCV replicon cells that is absent in naïve HuH-7 cells. This suggests that the antiserum is specific for NS5A and is capable of detecting NS5A in HCV replicon cells. However, the background staining was quite substantial (which is not obvious from Fig. 5.2 because the background was dimmed to darkness in HuH-7 cells).

In order to increase the specificity of the antiserum, the antiserum was purified by affinity chromatography.

5.1.3 Purification of the NS5A-specific antiserum.

In order to purify the antiserum by affinity chromatography, purified NS5A (211-449) (compare Fig. 5.1) was immobilized on activated NHS Sepharose. Coupling of NS5A (211-449) to the column material was monitored by silver staining.

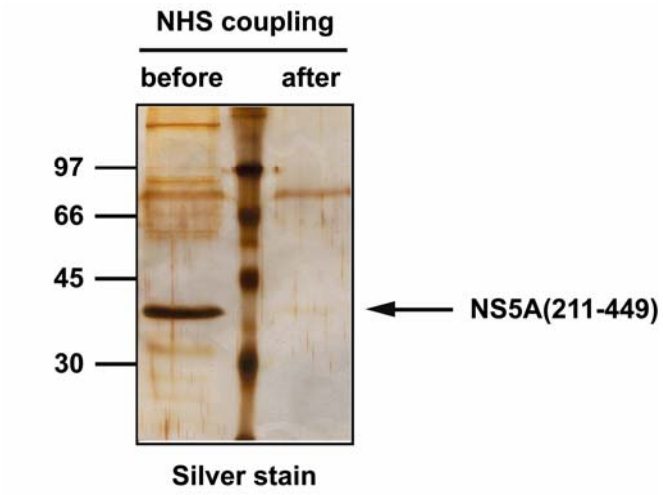

Fig. 5.3 NS5A (211-449) was efficiently coupled to NHS Sepharose. NS5A (211-449) was dialyzed against coupling buffer and incubated with acid-activated NHS Sepharose for 4h. Aliquots were taken before and after coupling of NS5A (211-449) to NHS Sepharose and analyzed by SDS-PAGE and subsequent silver staining.

Fig. 5.3 illustrates that purified NS5A (211-449) was efficiently coupled to NHS Sepharose. NHS Sepharose was subsequently washed to get rid of non-covalently- associated proteins and equilibrated with PBS.

The equilibrated affinity chromatography column displaying NS5A(211-449) was then loaded with 10ml of the NS5A-specific antiserum. Antibodies that bound to the affinity chromatography column were eluted by a pH shift (pH 2.7).

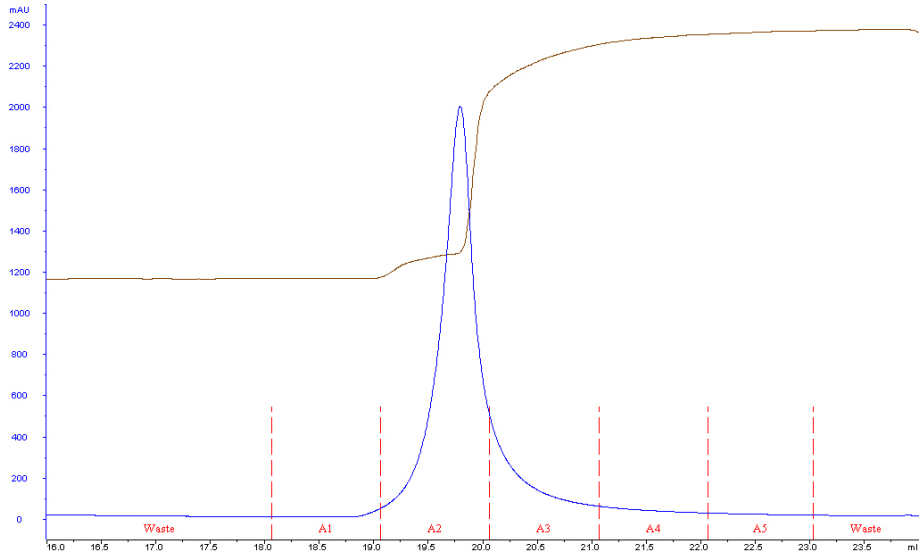

Fig. 5.4 Purification of the NS5A-specific antiserum by affinity chromatography. The rabbit-derived antiserum was loaded on an affinity column displaying NS5A(211-449). Bound antibodies were eluted by a pH shift (pH 2.7). Absorption at 280nm (protein) is displayed in blue. Conductivity is displayed in brown.

Fig. 5.4 shows that upon the shift of the pH, a distinct protein peak of almost 2000mAU is eluted from the column. This peak is essentially contained in the eluate fraction A2. It represents the purified antiserum. Elution of the antiserum is preceded by a shift in conductivity (brown) that reflects the difference in ionic strength between loading buffer and elution buffer.

The eluate fraction A2 was analyzed for its potential to detect NS5A expression in HCV replicon cells as described in Fig. 5.2.

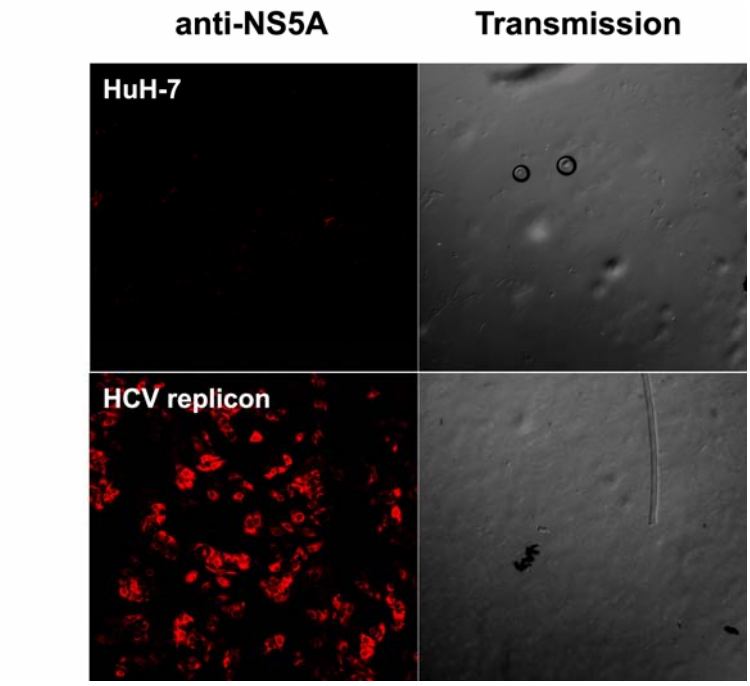

Fig. 5.5 Specificity of the NS5A-specific antiserum was strongly increased by purification. HCV replicon cells HuH-7 I_{377}/NS3-3`/wt/9-13 or naïve HuH-7 cells were fixed in ethanol and stained with the purified NS5A-specific antiserum (eluate fraction A2). NS5A was visualized using Cy3-coupled secondary antibody. Samples were analyzed by confocal laser scanning microscopy (Magnification 100X).

As seen in Fig. 5.5, purification of the NS5A-specific antiserum strongly increased the specificity of this antiserum. This may be due to an enrichment of NS5A-specific antibodies and a reduction of background staining at the same time. Again, the latter is not evident from the confocal images because the background in HuH-7 cells was again dimmed to darkness.

It is noteworthy that HCV replicon cells display a quite heterogeneous expression of NS5A with some cells expressing large amounts of NS5A and others being almost devoid of NS5A. This was an unexpected finding that was further analyzed as described in chapter 5.3.1.

5.2 Identification of c-Raf1 as a novel binding partner of NS5A.

5.2.1 Purification of NS5A

As mentioned above, purification of full-length NS5A turned out to be more difficult than purification of NS5A(211-449). This was mainly due to differences in the expression level and the solubility (data not shown).

Full-length NS5A was purified from a bacterial expression system. In brief, NS5A was expressed as a fusion protein with an N-terminal Step tag and a C-terminal V5 epitope (Strep-NS5A-V5). Strep-NS5A-V5 was purified by *Strep*Tactin Sepharose chromatography in presence of 0.5% NP-40 according to the manufacturer's instructions. The detergent was added to solubilize the otherwise membrane-associated protein (Huang et al., 2004). Purified eluate fractions (E2-E5) were subjected to SDS-PAGE and analyzed by silver staining or by Western blotting using a V5-specific antibody.

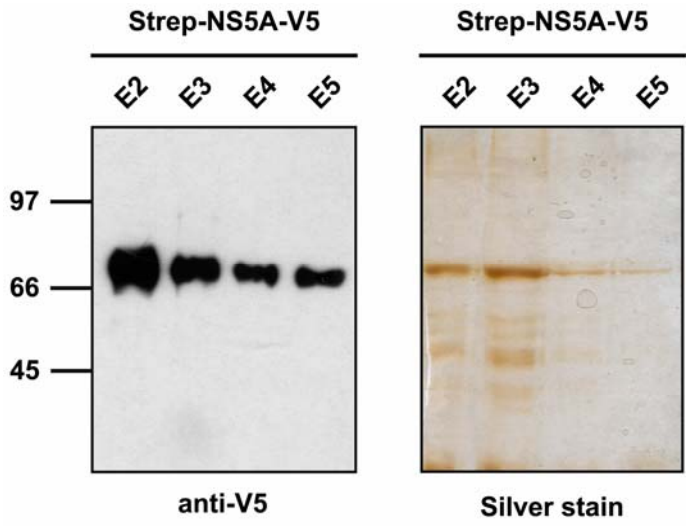

Fig. 5.6 *E.coli*-derived full-length NS5A is purified by *Strep*Tactin Sepharose chromatography. Strep-NS5A-V5 was expressed in *E.coli* using the bacterial expression plasmid pASK-IBA7-NS5A-V5. Bacteria were lysed in the presence of 0.5% NP-40. Strep-NS5A-V5 was purified by *Strep*Tactin Sepharose chromatography according to the manufacturer's instructions. Eluate fractions (E2-E5) were analyzed by Western blotting using a V5-specific antibody (Invitrogen) or by silver staining.

Fig. 5.6 shows that Strep-NS5A-V5 was expressed in *E.coli* and purified by *Strep*Tactin Sepharose chromatography. The silver stained SDS-PAGE documents that NS5A was obtained at high purity. Especially the late eluate fractions (E4, E5) contained highly purified NS5A. The Western blot confirms the identity of the Strep-NS5A-V5.

In summary, *E.coli*-derived Strep-NS5A-V5 could be purified by *Strep*Tactin Sepharose chromatography. However, since NS5A does not possess any catalytical activity, proper folding of the *E.coli*-derived NS5A could not be assessed. Therefore, NS5A was also expressed in Sf21 cells by the means of a recombinant baculovirus that codes for Strep-NS5A-V5. The recombinant baculovirus was generated as described in chapter 4.2.3. Sf21-derived Strep-NS5A-V5 was also purified by *Strep*Tactin Sepharose. However, the yield for Sf21-derived Strep-NS5A-V5 was significantly lower than for the *E.coli*-derived protein (data not shown).

5.2.2 c-Raf1 binds to immobilized NS5A.

In order to identify novel binding partners of NS5A, purified Strep-NS5A-V5 derived from Sf21 cells was immobilized on a *Strep*Tactin Sepharose column (Fig. 5.7A). Immobilized NS5A was loaded with cell lysate derived from human hepatoma cells (HuH-7) to allow potential interaction partners to bind to the column. Strep-NS5A-V5 was eluted from the column and the eluates were analyzed for coeluted proteins by Western blotting. As a negative control, a fusion protein of Hepatitis B Virus Core (HBc) with an N-terminal *Strep* tag was included and treated accordingly. To determine unspecific binding of proteins derived from HuH-7 cells to the column material, a separate column was incubated with HuH-7 cell lysate without loading any Sf21-derived proteins at all. The eluates were analyzed for coelution of proteins involved in the MAP kinase signaling cascade.

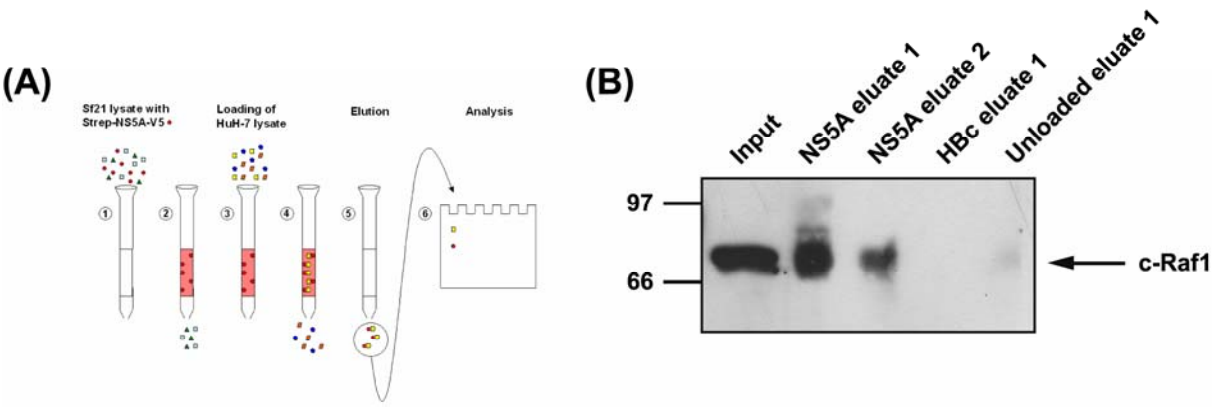

Fig. 5.7 c-Raf1 binds to immobilized NS5A. (A) Schematic representation: (1) A fusion protein of NS5A with an N-terminal *Strep* tag and a C-terminal V5 epitope (Strep-NS5A-V5, red) was produced by infection of Sf21 cells with a recombinant baculovirus. (2) Strep-NS5A-V5 was immobilized on a *Strep*Tactin Sepharose column. (3) The column was incubated with hepatoma cell lysate (HuH-7). (4) Interaction partners of NS5A (yellow) that are present in the hepatoma cell lysate bind to the immobilized NS5A. (5) Strep-NS5A-V5 is eluted from the column. Potential interaction partners are coeluted. (6) Eluates are analyzed by SDS-PAGE and Western blotting. (B) The method depicted in (A) was applied for Strep-NS5A-V5. As a negative control, an unrelated protein (Strep-HBV-Core) was produced in Sf21 cells and treated accordingly. Moreover, an unloaded column was incubated with HuH-7 cell lysate only to monitor unspecific binding to the column material. The eluate was analyzed by Western blotting using a c-Raf1 specific antiserum (Santa Cruz).

As seen in Fig. 5.7B, c-Raf1 is present in the NS5A eluate fractions E1 and E2 (with E1 being the most concentrated fraction), but neither in the HBc fraction E1 nor in the unloaded fraction E1. This indicates that c-Raf1 binds specifically to the NS5A-loaded column and not to the control columns.

5.2.3 NS5A and c-Raf1 can be coimmunoprecipitated from Sf21 cells.

Fig. 5.7 suggested that NS5A interacts with c-Raf1 *in vitro*. However, it did not allow any conclusions as to whether NS5A binds to c-Raf1 in living cells. Sf21-derived c-Raf1 could not be detected using antisera directed against human c-Raf1 (data not shown). Therefore, NS5A and c-Raf1 were expressed by double infection of Sf21 cells with recombinant baculoviruses coding for Strep-NS5A-V5 and GST-Raf fusion proteins. 48h post infection, cell lysates were prepared and subjected to immunoprecipitation using c-Raf1- or NS5A-specific antisera. The precipitates were analyzed by Western blotting.

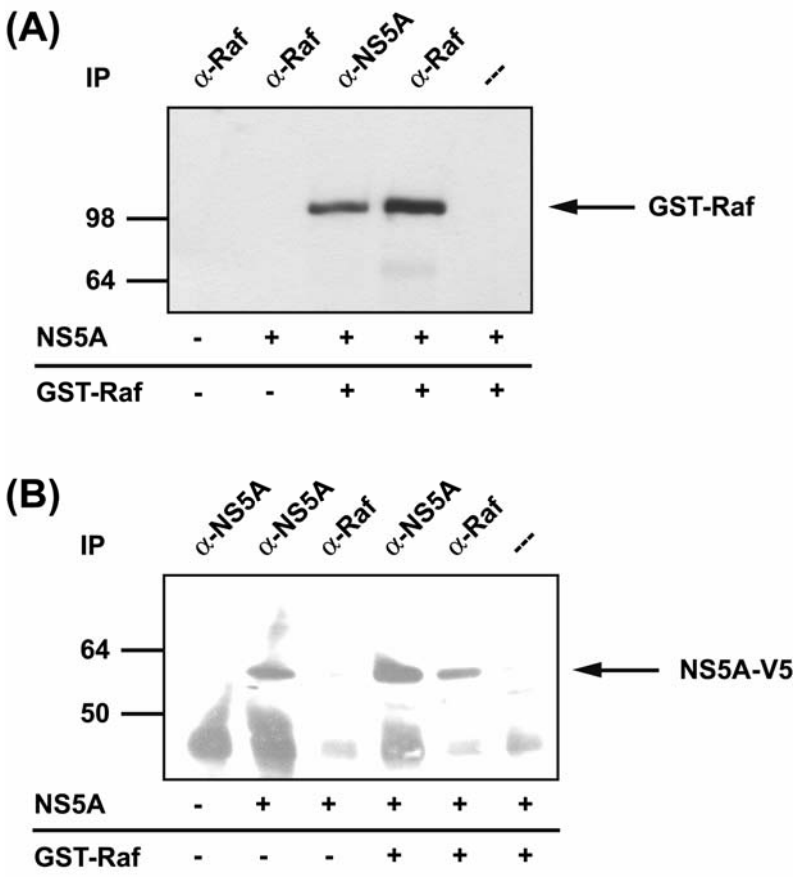

Fig. 5.8 NS5A and c-Raf1 are coimmunoprecipitated from Sf21 cells. Sf21 cells were infected with recombinant baculoviruses coding for NS5A or GST-Raf as indicated on the bottom. Infected cells were harvested 48h post infection and subjected to immunoprecipitation using NS5A- and c-Raf1-specific antisera as indicated. Precipitates were analyzed by Western blotting using a c-Raf1-specific antiserum (BD Transduction Laboratories) (A) or a V5-specific antibody (Invitrogen) (B).

Fig. 5.8A shows that GST-Raf is only detected when the Sf21 cells had been infected with a recombinant baculovirus coding for GST-Raf. Further more, GST-Raf is readily detected after precipitation with a c-Raf1-specific antiserum (α-Raf) and is absent when the precipitation was carried out in the absence of antiserum (---), indicating that the experimental conditions were suitable for specific immunoprecipitation of c-Raf1. Most importantly, c-Raf1 was also precipitated using an NS5A-specific antiserum, arguing that c-Raf1 and NS5A are coprecipitated. On the other hand, NS5A is also coimmunoprecipitated with GST-Raf (Fig. 5.8B). Again,

positive and negative controls included in this experiment suggest that the coimmunoprecipitation is specific.

In summary, these experiments demonstrate that NS5A binds to c-Raf1 in living cells.

5.2.4 c-Raf1 is colocalized with NS5A in the replication complex.

HCV selectively infects liver cells. Therefore, it was important to know whether the interaction of NS5A and c-Raf1 was also observed in a human liver cell line. To analyze this question, HuH-7 cells were transiently transfected with a eukaryotic expression plasmid coding for an NS5A fusion protein with an N-terminal HA- and a C-terminal V5-epitope (pcDNA-HA-NS5A-V5). Transfected cells were fixed 48h post transfection and stained with an HA-specific antiserum and a c-Raf1-specific antiserum to determine a potential colocalization of NS5A with endogenous c-Raf1. Samples were analyzed by confocal laser scanning microscopy.

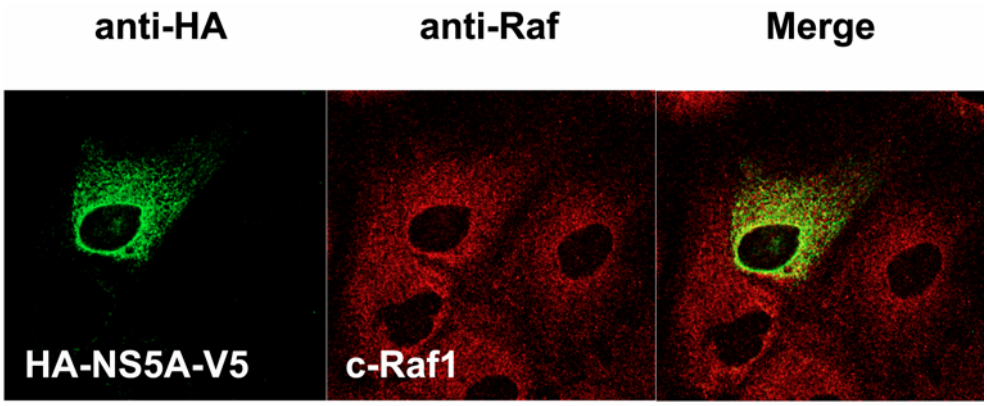

Fig. 5.9 NS5A is colocalized with endogenous c-Raf1. HuH-7 cells were transiently transfected with pcDNA-HA-NS5A-V5. Cells were fixed with cold ethanol 48h post transfection and stained with an HA-specific antiserum derived from rabbit (Santa Cruz) and a c-Raf1-specific antiserum derived from mouse (BD Transduction Laboratories). Samples were analyzed by confocal laser scanning microscopy (Magnification 600X).

As depicted in Fig. 5.9, NS5A displays a perinuclear localization whereas c-Raf1 is more evenly distributed in the cytosol with an enrichment in the perinuclear region. Both proteins are colocalized in the perinuclear region of HuH-7 cells.

However, in Fig. 5.9, NS5A expression was driven by the CMV promoter, leading to over-expression of NS5A. In order to evaluate whether NS5A was colocalized with c-Raf1 in a more

physiological setting, HCV replicon cells were analyzed. In these cells, HCV replication takes place in a cellular compartment that was recently defined by ultrastructural analysis and designated the "membranous web" (Gosert et al., 2003). Replication complexes contain the non-structural proteins of HCV, the viral RNA and cellular factors required for replication. To analyze whether c-Raf1 is present in the HCV replication complex, HCV replicon cells were fixed with 4% paraformaldehyde and stained with an NS5A-specific antiserum and a c-Raf1-specific antiserum. Samples were analyzed by confocal laser scanning microscopy.

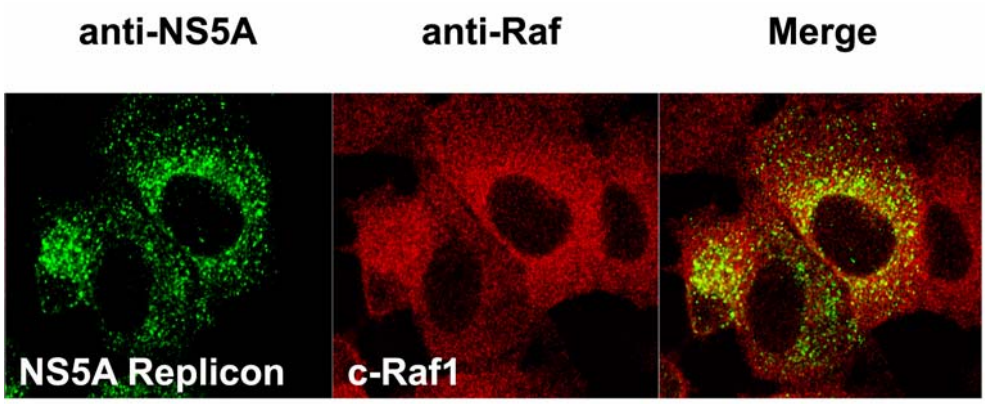

Fig. 5.10 c-Raf1 is colocalized with the HCV replication complex. HCV replicon cells HuH-7 I_{377}/NS3-3`/wt/9-13 were fixed with 4% paraformaldehyde and stained with an NS5A-specific antiserum derived from rabbit and a c-Raf1-specific antiserum derived from mouse (BD Transduction Laboratories). Samples were analyzed by confocal laser scanning microscopy (Magnification 600X).

As seen in Fig. 5.10, NS5A shows the typical perinuclear staining that is observed for all proteins in the HCV replication complex. However, in contrast to Fig. 5.9, NS5A displays a more punctuate staining that is only preserved by paraformaldehyde fixation (and not by ethanol fixation). These dot-like structures have been shown to contain the HCV replication complex (Gosert et al., 2003). Again, c-Raf1 is more evenly distributed in the cytosol with an enrichment in the perinuclear region. The merge image suggests that c-Raf1 is colocalized with the HCV replication complex. In addition, areas that display an elevated NS5A concentration also show local accumulation of c-Raf1, arguing that the localization of c-Raf1 depends on the localization of NS5A.

In summary, these experiments indicate that the interaction between c-Raf1 and NS5A is not only observed in Sf21 cells, but is also relevant in human hepatoma cells and in HCV replicon cells.

5.2.5 NS5A interacts with the catalytical domain of c-Raf1.

To analyze the interaction of c-Raf1 and NS5A in more detail, deletion mutants of the two proteins were generated. Intracellular localization of these mutants was determined by immunofluorescence microscopy. To that end, HuH-7 cells were transfected with an expression vector coding for a dominant-negative mutant of c-Raf1 that lacks the catalytical domain of c-Raf1 (Raf C4) (Bruder et al., 1992). Raf C4 is exclusively found in the nucleus. If this mutant was still able to bind to NS5A, this should either alter the perinuclear localization of NS5A or the nuclear localization of Raf C4.

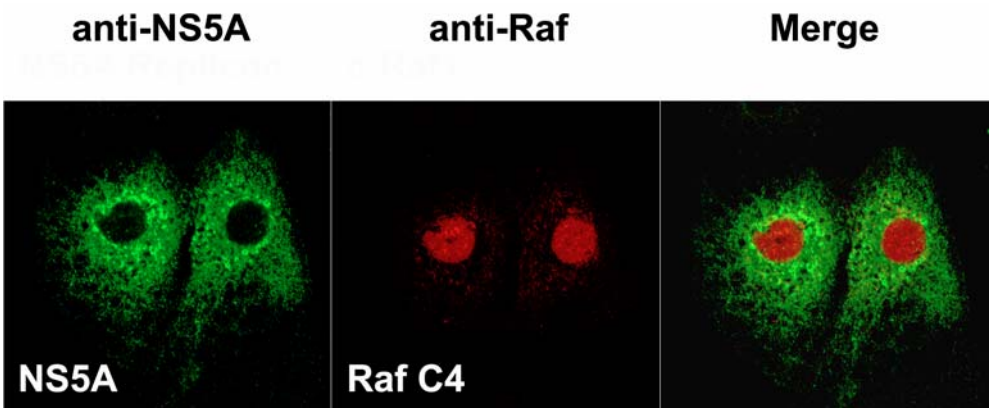

Fig. 5.11 NS5A is not colocalized with Raf C4. HuH-7 cells were transfected with pcDNA-HA-NS5A-V5 and pRK5-Raf C4. NS5A was detected using a V5-specific antiserum derived from rabbit (Sigma). Raf C4 was detected using a c-Raf1-specific antibody derived from mouse (BD Transduction Laboratories). Samples were analyzed by confocal laser scanning microscopy (Magnification 600X).

As seen in Fig. 5.11, localization of NS5A was unaffected by the presence of Raf C4 and vice versa, indicating that this mutant is no longer able to interact with NS5A. This argues for NS5A interacting with c-Raf1 in the catalytical domain of the latter.

On the other hand, a stepwise deletion of the N-terminal domain of NS5A was performed (NS5A 105-449, NS5A 211-449). It has been shown previously that N-terminal deletion mutants

of NS5A that lack the characteristic amphipathic helix are found in the nucleus (Brass et al., 2002). The NS5A deletion mutants described above were predominantly found in the nucleus, confirming the previously reported data. If those mutants still contained the c-Raf1 binding domain, the presence of these mutants may alter the cytoplasmic localization of c-Raf1.

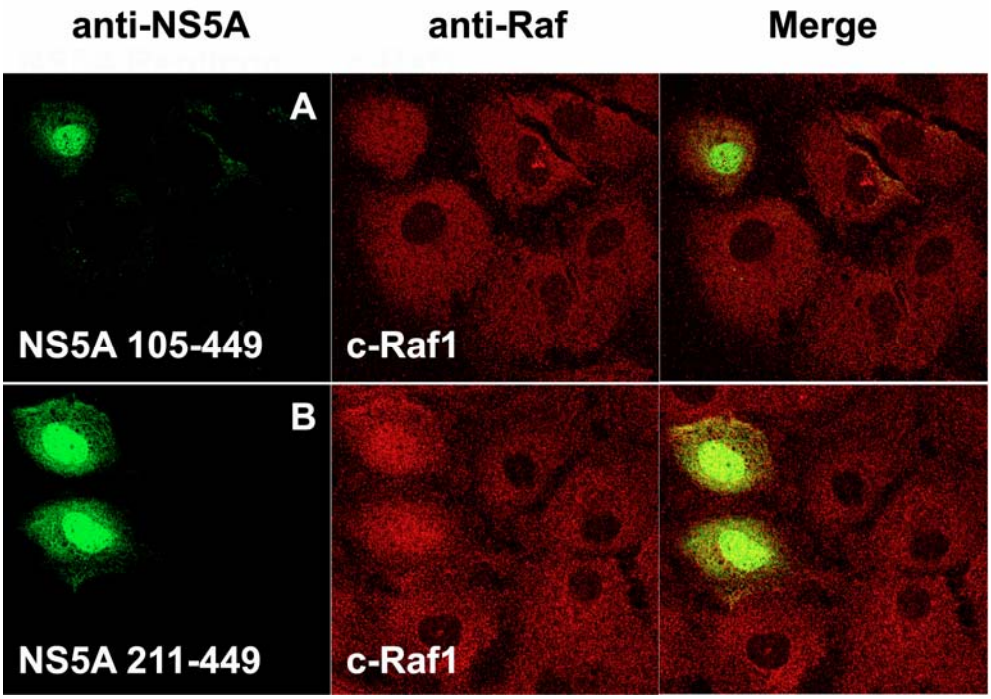

Fig. 5.12 c-Raf1 binds to the C-terminal half of NS5A (amino acids 211-449). HuH-7 cells were transfected with pcDNA-Strep-NS5A(105-449)-V5 (A) or pcDNA-Strep-NS5A(211-449)-V5 (B). NS5A was detected using a V5-specific antiserum derived from rabbit (Sigma). Endogenous c-Raf1 was detected using a c-Raf1-specific antibody derived from mouse (BD Transduction Laboratories). Samples were analyzed by confocal laser scanning microscopy (Magnification 600X).

Fig. 5.12 shows that nuclear localization of NS5A deletion mutants causes the translocation of endogenous c-Raf1 from the cytosol to the nucleus. Control experiments with an unrelated cytosolic protein (14-3-3) indicate that the nuclear translocation is specific for c-Raf1 (data not shown). Given the fact that, in the absence of NS5A deletion mutants, c-Raf1 is exclusively localized in the cytosol, the interaction of these two proteins must be quite strong. Furthermore, these data indicate that both NS5A 105-449 and NS5A 211-449 are able to bind to c-Raf1, arguing that c-Raf1 binds to the C-terminal half of NS5A.

5.3 MAP kinase signaling and HCV replication.

5.3.1 Initial characterization of HCV replicon cells.

The study of viral life cycle of HCV is hampered by the fact that HCV does not infect cultured cells. The only surrogate model that is currently available is the replicon model (Lohmann et al., 1999). This model system is based on subgenomic HCV RNA that replicates autonomously after transfection of HuH-7 cells.

The following experiments were performed with two HCV replicon cell lines, both of which are highly adapted to cell culture conditions. HuH-7 I_{377}/NS3-3`/wt/9-13 cells harbour a replicon RNA that contains an adaptive mutation in NS5B (R2884G) (Lohmann et al., 1999). HuH-7 $I_{389}$/NS3-3`/LucUbiNeo-ET cells harbour a replicon RNA that contains adaptive mutations in NS3 (E1202G, T1280I) and NS4B (K1848I) (Frese et al., 2003). Whereas the former have retained NS5A hyperphosphorylation, the latter have lost it due to the cell culture adaptation. However, the latter are particularly suitable for analysis of HCV replication since the replicon RNA harbours a luciferase gene. Luciferase gene expression is tightly correlated with HCV replication (Frese et al., 2003), allowing for the convenient analysis of HCV replication by measuring luciferase levels.

To initially characterize these cells, it was essential to know whether gene expression could be detected. Fig. 5.5 demonstrates that NS5A expression was readily detected in these cells. As described in chapter 5.1.3, NS5A expression was very heterogeneous with some cells expressing high amounts of NS5A and others expressing almost no NS5A whatsoever. In order to analyze whether the observed heterogeneity was restricted to NS5A, HCV replicon cells were also analyzed for expression of NS5B.

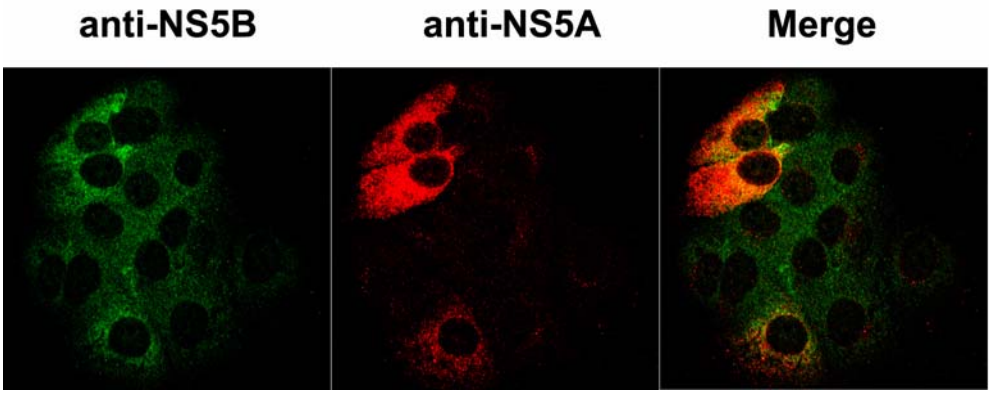

Fig. 5.13 NS5B and NS5A are heterogeneously distributed in HCV replicon cells. HCV replicon cells HuH-7 I_{377}/NS3-3`/wt/9-13 were fixed in ethanol and analyzed using an NS5B-specific monoclonal antibody derived from mouse and an NS5A-specific antiserum derived from rabbit. NS5B was visualized using a FITC-coupled secondary antibody, whereas NS5A was visualized using a Cy3-coupled secondary antibody. Samples were analyzed by confocal laser scanning microscopy (Magnification 600X).

Fig. 5.13 suggests that both NS5B and NS5A are heterogeneously distributed. Interestingly, the heterogeneous distribution of these two proteins is similar, ie. cells expressing high levels of NS5A also express high levels of NS5B. This argues that the observed differences originate on the RNA level (rather than on the protein level), implying that high levels of HCV gene expression result from high levels of viral RNA replication. Differences in viral replication could be due to the cellular environment or due to intrinsic properties of the viral RNA.

Although the immunofluorescence analysis confirms that HCV non-structural proteins could be detected in the HCV replicon cells, it did not allow any conclusions as to whether NS5A hyperphosphorylation was retained. Therefore, HCV replicon cells HuH-7 I_{377}/NS3-3`/wt/9-13 were lysed in SDS sample buffer and the lysate was analyzed by Western blotting using an NS5A-specific antiserum.

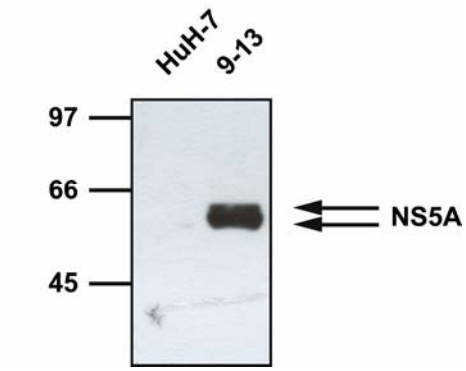

Fig. 5.14 NS5A migrates as a double band in an SDS-PAGE. HCV replicon cells HuH-7 I_{377}/NS3-3`/wt/9-13 were lysed in SDS sample buffer, electrophoresed on a 10% SDS-PAGE and analyzed by Western blotting using an NS5A-specific antiserum. Naïve HuH-7 cells were included as a negative control.

As seen in Fig. 5.14, NS5A expression was detected in HCV replicon cells but not in naïve HuH-7 cells. Furthermore, NS5A migrates as a double band in an SDS-PAGE (Blight et al., 2000). Fig. 5.14 illustrates that the NS5A double band is difficult to resolve. This may be due to the fact that the p58 species is not as prominent as the p56 species. In fact, p58 is only detected in very concentrated cell lysates that may be suboptimal in terms of electrophoretic separation. As predicted, p58 was only detectable in HuH-7 I_{377}/NS3-3`/wt/9-13 cells, but not in HuH-7 $I_{389}$/NS3-3`/LucUbiNeo-ET (data not shown).

In summary, these experiments show that the HCV replicon cell line HuH-7 I_{377}/NS3-3`/wt/9-13 produces detectable amounts of HCV non-structural proteins (NS5A and NS5B). Furthermore, NS5A hyperphosphorylation is retained in these cells.

5.3.2 BAY43-9006 inhibits the protein kinase C-induced activation of the MAP kinase cascade.

The experiments presented in chapter 5.2 demonstrate that c-Raf1 binds to NS5A in several experimental designs. If this interaction is relevant with regard to viral replication, an inhibition of c-Raf1 or its downstream effector MEK should affect the rate of viral replication. c-Raf1 and MEK were inhibited using small-molecule inhibitors: Whereas there is only one small-molecule inhibitor of c-Raf1 that is commercially available (BAY43-9006), there are at least two well-established small-molecule inhibitors of MEK (PD98059 and U0126). The c-Raf1 inhibitor

BAY43-9006 acts as a competitive inhibitor with regard to ATP (Lyons et al., 2001). On the contrary, PD09059 and U0126 are non-competitive with regard to the MEK substrates ERK and ATP (Dudley et al., 1995; Favata et al., 1998).

In order to assess the impact of these inhibitors on HCV replication, it was crucial to evaluate their inhibitory potential with regard to the MAP kinase pathway. To that end, HCV replicon cells were stimulated with phorbol 12-myristate 13-acetate (PMA), which is structurally similar to diacylglycerol (DAG). PMA binds to and activates protein kinase C, resulting in a profound stimulation of the MAP kinase cascade. This was detected on the level of MEK, ERK or AP-1. MEK and ERK activation were measured by Western blotting using phospho-MEK and phospho-ERK specific antibodies. AP-1 activation was determined in an AP-1-driven reporter gene assay using luciferase as a reporter gene. Specific inhibitors for c-Raf1 (BAY43-9006) or MEK (PD98059, U0126) were tested for their potential to reduce the PMA-induced stimulation of the MAP kinase cascade.

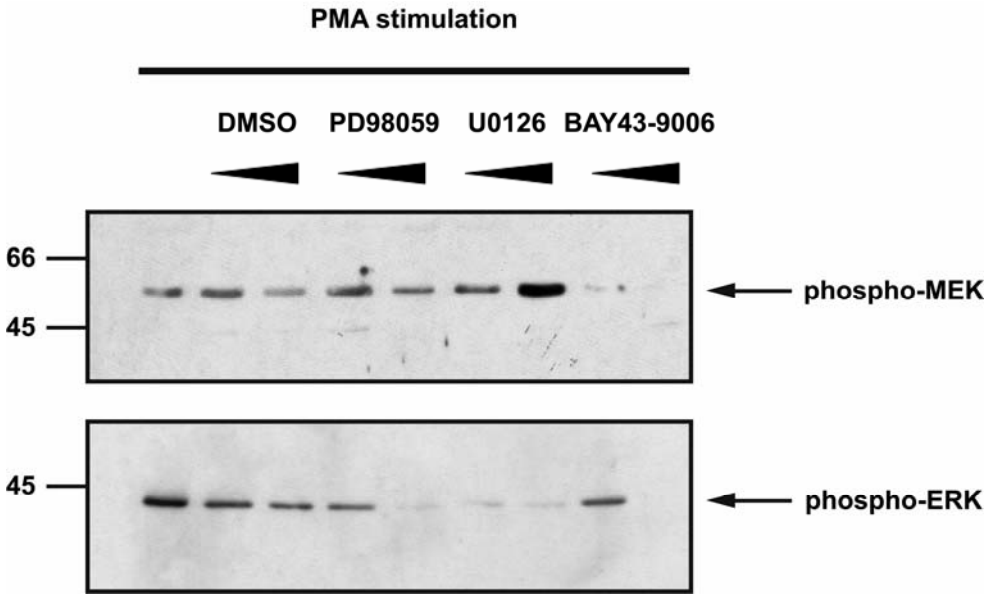

Fig. 5.15 BAY43-9006, PD98059 and U0126 are functional inhibitors of the MAP kinase cascade. HCV replicon cells HuH-7 I_{377}/NS3-3`/wt/9-13 were preincubated with DMSO (1%, 10%), PD98059 (5μM, 20μM), U0126 (1μM, 10μM) or BAY43-9006 (1μM, 10μM) for 30min. Cells were subsequently stimulated with 100ng/ml PMA for 20min. Cells were harvested in SDS sample buffer and lysates were analyzed by Western blotting using a phospho-MEK-specific antibody (Cell Signaling Technology) or a phospho-ERK-specific antibody (anti-active MAPK, Promega).

As seen in Fig. 5.15, PMA induced a robust phosphorylation of MEK and ERK. As expected, BAY43-9006 inhibits the PMA-induced phosphorylation of both MEK and ERK. This demonstrates that this inhibitor exerts its effect upstream of MEK, ie. at the level of c-Raf1. On the other hand, PD98059 and U0126 inhibit ERK phosphorylation without inhibiting MEK phosphorylation, arguing that they disrupt the MAP kinase cascade at the level of MEK.

To be able to quantify the inhibitory potential of BAY43-9006, an AP-1 reporter gene assay was performed. To that end, human hepatoma cells (HepG2) were transfected with an AP-1 reporter gene construct. 48h post transfection, cells were preincubated with BAY43-9006 at the indicated concentrations for 30min. and subsequently stimulated with PMA for 6h.

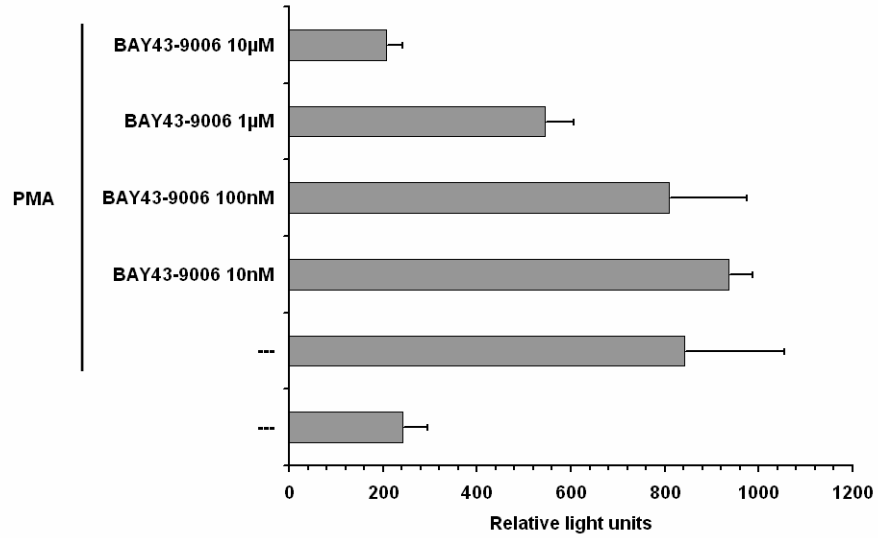

Fig. 5.16 BAY43-9006 inhibits the PMA-induced activation of AP-1 in a dose-dependent manner. HepG2 cells were preincubated with BAY43-9006 for 30min. at the indicated concentrations. Then, cells were stimulated with 100ng/ml PMA for 6h. Cells were harvested in reporter gene assay lysis buffer (Roche) and lysates were analyzed by automated addition of the luciferase substrate buffer and subsequent determination of chemoluminescence.

Fig. 5.16 shows that BAY43-9006 also inhibits the PMA-induced activation of AP-1. The IC_{50} was estimated to lie around 1µM in these cells. This is in agreement with Fig. 5.15 where BAY43-9006 shows a subtle inhibition at 1µM and profound inhibition at 10µM.

PD98059 and U0126 were also analyzed for their potential to inhibit the PMA-induced activation of AP-1 (data not shown). Whereas PD98059 displays an IC_{50} of about 10μM, U0126 shows an IC_{50} of 1μM.

5.3.3 Inhibition of c-Raf1 by BAY43-9006 negatively affects HCV replication.

The experiments depicted in Fig. 5.15 and Fig. 5.16 demonstrate that BAY43-9006 was functional in terms of disrupting the MAP kinase cascade. Complete inhibition of c-Raf1 was obtained at 10μM BAY43-9006. In order to analyze the consequence of c-Raf1 inhibition for HCV replication, HCV replicon cells HuH-7 I_{389}/NS3-3`/LucUbiNeo-ET were incubated with 10μM BAY43-9006 or equivalent quantities of the solvent (DMSO) for 6h. Cells were harvested immediately thereafter and HCV replication was analyzed by measuring luciferase levels.

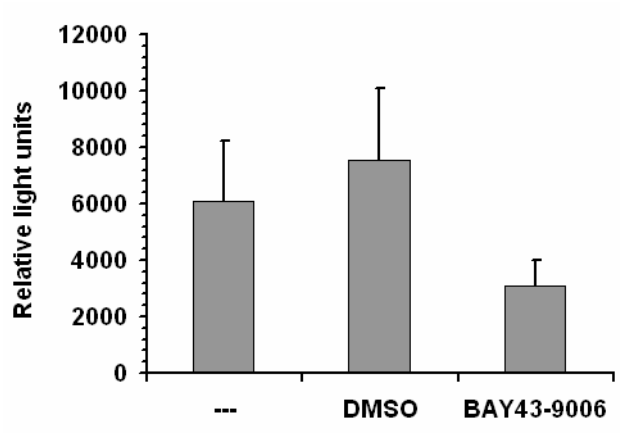

Fig. 5.17 Inhibition of c-Raf1 by BAY43-9006 leads to a decrease in HCV replication. HCV replicon cells HuH-7 I_{389}/NS3-3`/LucUbiNeo-ET were incubated with DMSO (1%) or BAY43-9006 (10μM) for 6h. Cells were harvested immediately thereafter and HCV replication was analyzed by measuring luciferase levels.

Fig. 5.17 demonstrates that inhibition of c-Raf1 by the small molecule inhibitor BAY43-9006 leads to a significant decrease in HCV replication whereas DMSO does not significantly affect HCV replication. This argues that the integrity of c-Raf1 is essential for viral replication.

5.3.4 BAY43-9006-mediated inhibition is not due to a block in cell proliferation.

HCV replication in HCV replicon cells is tightly coupled to the proliferation state of the host cell (Pietschmann et al., 2001): HCV replicates to high levels in proliferating cells and replication is dramatically reduced once the cells reach confluency. c-Raf1 is a kinase that is critically involved in the regulation of cell growth and proliferation. Therefore, a blockade of c-Raf1 might simply cause a cell-cycle arrest and HCV replication may drop as a consequence of that. To exclude that a block in cell proliferation is the major reason underlying the BAY43-9006-mediated decrease in HCV replication, HCV replicon cells were incubated with 10µM BAY43-9006 and 1mM hydroxyurea in parallel. Hydroxyurea inhibits ribonucleotide reductase and thereby blocks cell proliferation. To document the effect of hydroxyurea on cell proliferation, cells were counted in parallel.

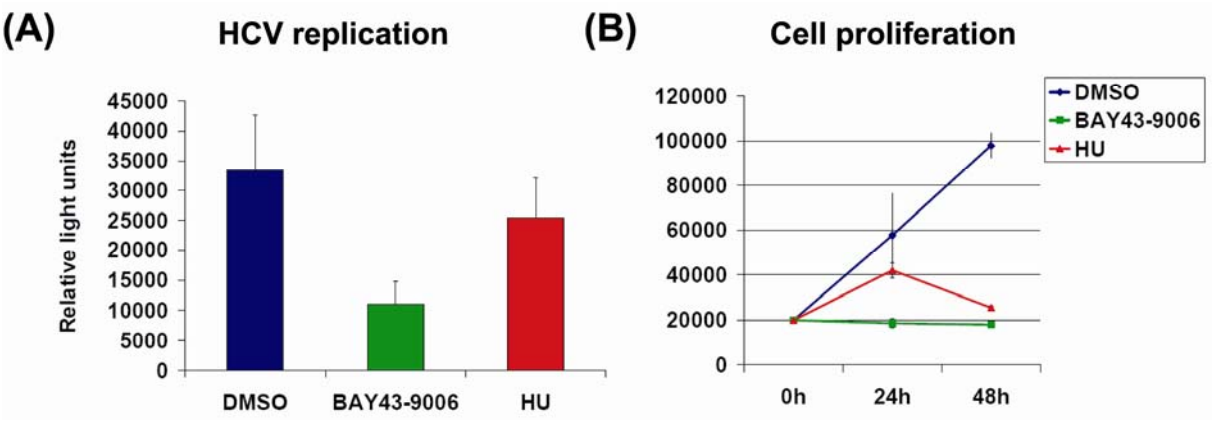

Fig. 5.18 BAY43-9006 blocks HCV replication whereas hydroxyurea (HU) does not. (A) HCV replicon cells HuH-7 I_{389}/NS3-3`/LucUbiNeo-ET were incubated with 1% DMSO, 10µM BAY43-9006 or 1mM hydroxyurea (HU) for 6h. Cells were harvested immediately thereafter and replication was analyzed by measuring luciferase levels. (B) HCV replicon cells HuH-7 $I_{389}$/NS3-3`/LucUbiNeo-ET were incubated with 1% DMSO, 10µM BAY43-9006 or 1mM hydroxyurea (HU) for the indicated time periods (24h/48h). Cells were harvested by trypsination and counted.

Fig. 5.18A shows that BAY43-9006 blocks HCV replication (as expected) whereas 1mM hydroxyurea (HU) does not significantly affect HCV replication when applied for 6h. At the same time, both 1mM hydroxyurea and 10µM BAY43-9006 significantly reduce cell proliferation when applied for 24 or 48h (Fig. 5.18B). This indicates that the BAY43-9006-mediated reduction in HCV replication is not simply due to a block in cell proliferation. However, BAY43-9006 and

hydroxyurea show different kinetics with regard to the block in cell proliferation (Fig. 5.18B): Whereas the BAY43-9006-mediated block in cell proliferation is detected at 24h, it takes at least 48h for hydroxyurea to significantly affect cell proliferation. Therefore, it cannot be excluded that the BAY43-9006-mediated decrease in HCV replication is at least partially due to a block in cell proliferation.

In summary, these experiments show that hydroxyurea does not affect HCV replication to the same extent as BAY43-9006, arguing that the decrease in HCV replication is not the simple consequence of a block in cell proliferation.

5.3.5 Downregulation of c-Raf1 by siRNA leads to a decrease in HCV replication.

To further substantiate the hypothesis that c-Raf1 is critically involved in HCV replication, c-Raf1 expression was reduced by the means of small interfering RNAs (siRNAs). HCV replicon cells were transfected with a c-Raf1-specific siRNA or a negative control siRNA. Replication was analyzed 48h post transfection.

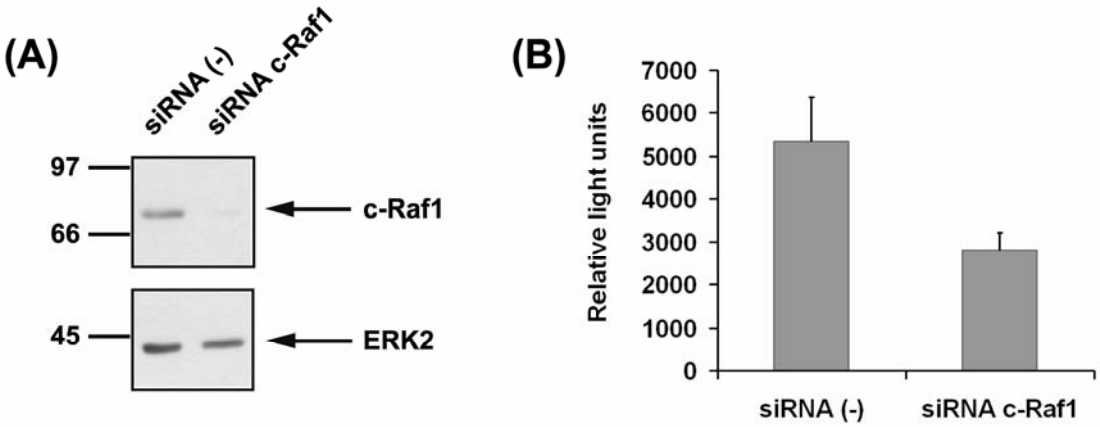

Fig. 5.19 Reduced expression of c-Raf1 leads to a decrease in HCV replication. (A) HCV replicon cells HuH-7 I_{389}/NS3-3`/LucUbiNeo-ET were transfected with a c-Raf1-specific siRNA or a negative control siRNA. c-Raf1 expression was monitored by Western blotting using a c-Raf1 specific antiserum (Santa Cruz). As a control, expression of ERK-2 was monitored using an ERK2-specific antiserum (Santa Cruz). (B) Cells were treated as described in (A) and HCV replication was analyzed by measuring luciferase levels.

To monitor the degree of downregulation of c-Raf1, c-Raf1 expression was analyzed by Western blotting using a c-Raf1-specific antiserum. Fig. 5.19A. shows that c-Raf1 expression is

significantly reduced whereas ERK2 expression is largely unaffected, arguing that the siRNA-mediated downregulation of c-Raf1 is specific. Fig. 5.19B shows that replication is modestly affected by the reduction of c-Raf1 expression. In agreement with Fig. 5.17, a loss of c-Raf1 expression leads to a decrease in HCV replication.

5.3.6 Inhibition of MEK by PD98059 positively affects HCV replication.

Fig. 5.17 and Fig. 5.19 suggest that integrity of c-Raf1 is essential for HCV replication. However, these experiments do not allow any conclusions about the mechanism of c-Raf1-mediated regulation of HCV replication. At least two scenarios are conceivable: (i) Integrity of the MAP kinase cascade (Raf/MEK/ERK) is essential for HCV replication. As a consequence, disruption of the MAP kinase cascade should always result in decreased HCV replication, no matter whether the signaling cascade is disrupted at the level of c-Raf1 or MEK. (ii) c-Raf1 exerts an effect that is independent of the MAP kinase cascade, e.g. by directly interacting with one or more viral proteins. In this case, disruption of the MAP kinase cascade at the level of MEK should not produce the same effect as disruption at the level of c-Raf1.

In order to distinguish between those two possibilities, HCV replicon cells were incubated with the MEK inhibitor PD98059. Again, if the BAY43-9006-mediated decrease in replication is essentially due to a decreased activation level of the MAP kinase cascade, the effect of PD98059 should be similar to the effect of BAY43-9006, ie. PD98059 should also decrease the level of HCV replication.

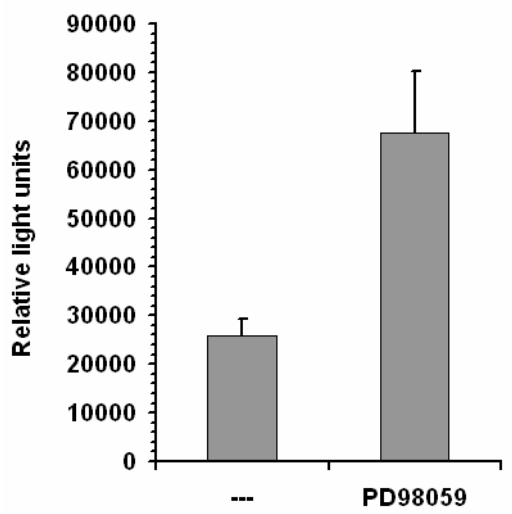

Fig. 5.20 Inhibition of MEK by PD98059 leads to an increase in HCV replication. HCV replicon cells HuH-7 I_{389}/NS3-3`/LucUbiNeo-ET were incubated with PD98059 (18μM) for 6h. Cells were harvested immediately thereafter and HCV replication was analyzed by measuring luciferase levels.

Surprisingly, incubation of HCV replicon cells with 18μM PD98059 leads to an increase in HCV replication (Fig. 5.20).

To further evaluate this unexpected finding, a different MEK inhibitor (U0126) was used in the same experimental design. U0126 displays a higher affinity for MEK than PD98059 and is said to be more specific than PD98059 at the same time (Favata et al., 1998). Again, HCV replicon cells were incubated with 10μM U0126 or with the equivalent amount of solvent (DMSO).

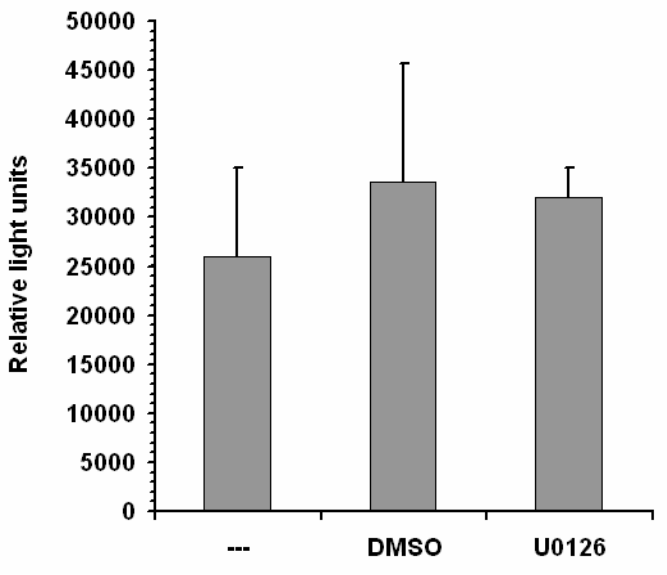

Fig. 5.21 U0126 does not affect HCV replication. HCV replicon cells HuH-7 I_{389}/NS3-3`/LucUbiNeo-ET were incubated with U0126 (10μM) or DMSO (1%) for 6h. Cells were harvested immediately thereafter and HCV replication was analyzed by measuring luciferase levels.

Incubation of HCV replicon cells with 10μM U0126 did not alter HCV replication at all (Fig. 5.21) although U0126 inhibited ERK phosphorylation to the same extent as PD98059 (compare Fig. 5.15). This indicates that the effect of PD98059 on HCV replication is not due to the inhibition of MEK.

Although the experiments with PD98059 and U0126 are not fully conclusive with regard to the role of MEK in HCV replication, they provide evidence for scenario (ii) that proposes a role for c-Raf1 in HCV replication that is not directly related to its downstream effectors MEK or ERK.

In summary, these experiments show that integrity of c-Raf1 is essential for HCV replication. Furthermore, the BAY43-9006-mediated decrease in HCV replication is not due to a block in cell proliferation. A blockade at the level of MEK does not result in a similar decrease in HCV replication, arguing that the role of c-Raf1 in HCV replication is not coupled to the activation of its downstream substrate MEK. In contrast, these experiments suggest a rather exclusive role for c-Raf1 in HCV replication.

5.4 NS5A does not alter c-Raf1-mediated signal transduction.

5.4.1 NS5A does not affect ERK phosphorylation.

The results presented in chapter 5.2 suggest that c-Raf1 binds to NS5A in several experimental designs. Furthermore, inhibition of c-Raf1 by the means of a small-molecule inhibitor or by siRNA leads to a decrease in HCV replication (chapter 5.3.3), indicating that c-Raf1 interferes with viral replication. On the other hand, binding of NS5A to c-Raf1 may also affect the activity of c-Raf1. As a consequence, signaling cascades downstream of c-Raf1 should be modulated by the presence of NS5A. The most prominent downstream effector of c-Raf1 is the MAP kinase cascade Raf/MEK/ERK. ERK lies downstream of c-Raf1 and becomes phosphorylated upon c-Raf1 activation. Phosphorylation of ERK can be visualized using a phospho-ERK specific antibody. In order to analyze whether the presence of NS5A affects the level of activation of the MAP kinase cascade, HCV replicon cells were compared to naïve HuH-7 cells with regard to ERK phosphorylation. Cells were either left untreated or stimulated with PMA.

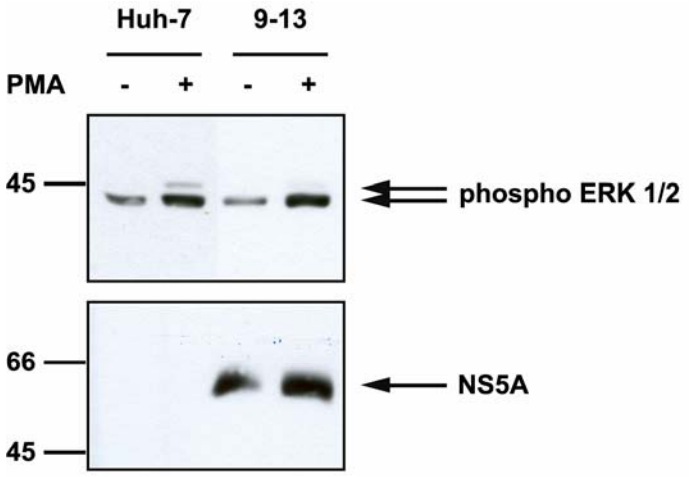

Fig. 5.22 ERK phosphorylation is not altered in HCV replicon cells. HuH-7 cells or HCV replicon cells HuH-7 I_{377}/NS3-3`/wt/9-13 were stimulated with PMA for 20min. as indicated. Cells were harvested and lysates were analyzed by Western blotting using either a phospho-ERK-specific antibody (anti-active MAPK, Promega) or an NS5A-specific antiserum.

Fig. 5.22 shows that ERK phosphorylation in HCV replicon cells is similar to naïve HuH-7 cells. Further more, PMA-induced activation of the MAP kinase cascade (Raf/MEK/ERK) is not

altered by the presence of NS5A either. NS5A expression was verified by Western blotting using an NS5A-specific antiserum. This experiment suggests that NS5A does neither exert a positive nor a negative effect on ERK phosphorylation.

5.4.2 NS5A does not modulate the activity of SRF, AP-1, NF-κB or STAT-3

The experiment presented in the previous chapter indicates that NS5A does not affect the level of c-Raf1 activity. However, the NS5A-mediated activation of the MAP kinase cascade might be very subtle and therefore undetectable at the level of ERK phosphorylation. Nevertheless, a weak effect at the level of ERK may be amplified by the signal transduction cascade, leading to a more robust signal at the level of transcription factor activation. The most prominent transcription factor downstream of the MAP kinase cascade Raf/MEK/ERK is the serum response factor (SRF) (Chai and Tarnawski, 2002). Therefore, it was investigated whether NS5A affects the activation level of SRF.

On the other hand, NS5A targets a number of transcription factors and modulates their activity. Those include AP-1 (Macdonald et al., 2003), NF-κB and STAT-3 (Gong et al., 2001). Since c-Raf1 is a pleiotropic molecule that affects several cellular signaling cascades, c-Raf1 may contribute to the NS5A-mediated modulation of these transcription factors. In fact, the c-Raf1/NS5A interaction may be causative for some of the effects previously ascribed to NS5A. In order to analyze the contribution of c-Raf1 to NS5A-mediated modulation of AP-1, NF-κB or STAT-3, it was necessary to confirm the effect of NS5A on these factors in the first place.

To that end, HuH-7 cells were transiently transfected with a eukaryotic expression plasmid coding for NS5A (pcDNA-NS5A) in the presence of different reporter plasmids harbouring *Photinus pyralis* luciferase as a reporter gene. *Photinus pyralis* luciferase expression was driven by SRF-, AP-1-, NF-κB- and STAT-3-dependent promoters. As a negative control, HuH-7 cells were transiently transfected with pcDNA-NS5A *inverse*. This plasmid contains the NS5A coding sequence in 3'-5' orientation, leading to the expression of a nonsense mRNA. To monitor transfection efficiency, HuH-7 cells were cotransfected with a reporter plasmid harbouring *Renilla reniformis* luciferase as a reporter gene. *Renilla reniformis* luciferase expression was driven by the Herpes Simplex Virus thymidine kinase (HSV-TK) promoter that is constitutively active. *Photinus pyralis* luciferase levels were normalized with regard to *Renilla reniformis* luciferase levels.

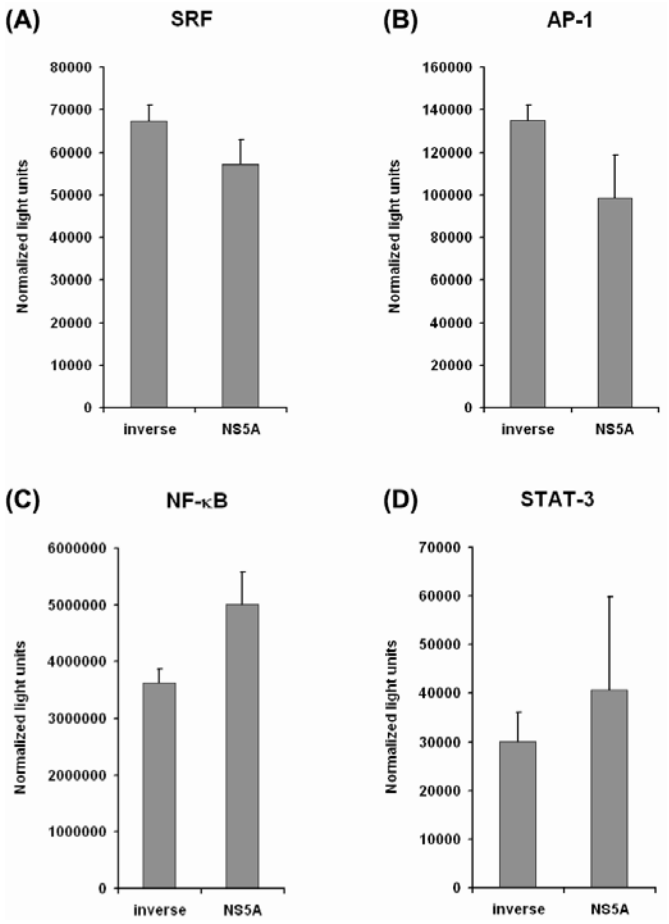

Fig. 5.23 NS5A does not alter the transcriptional activation of SRF, AP-1, NF-κB or STAT-3. HuH-7 cells were transfected with 1μg pcDNA-NS5A or pcDNA-NS5A *inverse* as indicated. 0.3μg of pSRE-Luc (A), pAP-1-Luc (B), pNF-κB-Luc (C) or pSTAT3-TA-Luc (D) were cotransfected as indicated. 0.3μg of pRL-TK was cotransfected with all samples and served as an internal reference. Cells were harvested 48h post transfection and analyzed by measuring both *Photinus pyralis* and *Renilla reniformis* luciferase levels using the Dual-Luciferase Reporter Assay System according to the manufacturer's instructions.

Fig. 5.23A shows that NS5A does not significantly alter the level of activation of the transcription factors SRF. This is in agreement with the data presented in Fig. 5.22 and suggests that the activity of the MAP kinase cascade is not significantly affected by the presence of NS5A.
Furthermore, NS5A does not modulate AP-1, NF-κB or STAT-3 activation either (Fig. 5.23 B,C,D). This is surprising, given the fact that at least NF-κB and STAT-3 have been shown to be activated by NS5A (Gong et al., 2001).

In order to ascertain proper expression of NS5A, lysates analyzed by luciferase assay (Fig. 5.23) were subjected to SDS-PAGE and Western blotting using NS5A- or actin-specific antisera.

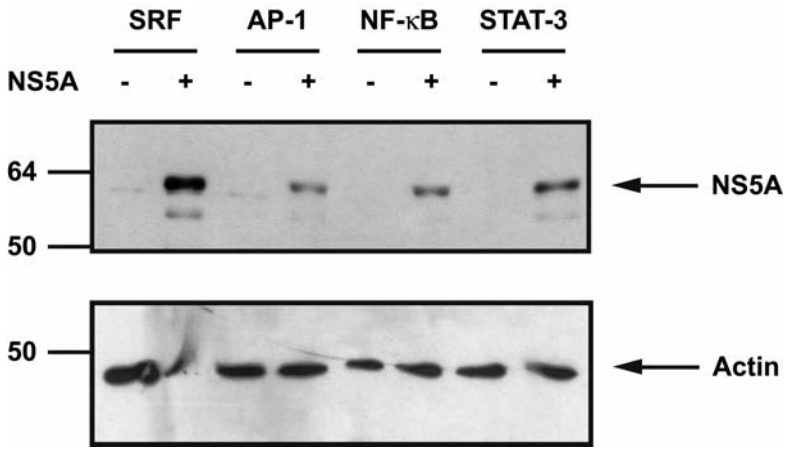

Fig. 5.24 NS5A is properly expressed after transient transfection of HuH-7 cells. HuH-7 cells were transfected as described in Fig. 5.23. Lysates were subjected to SDS-PAGE and Western blotting using an NS5A-specific antiserum or an actin-specific antiserum (Sigma).

Fig. 5.24 illustrates that NS5A was properly expressed in the samples that were analyzed in the reporter gene assay. This suggests that the absence of an NS5A-mediated effect on cellular signal transduction is not caused by a lack of NS5A expression.

5.4.3 HCV replicon cells do not differ from naïve HuH-7 cells with regard to SRF-, AP-1-, NF-κB- or STAT-3-activation.

In the experimental design presented in the previous chapter, NS5A was expressed as a single protein in the absence of the HCV polyprotein context. As mentioned before, NS5A is modified in the presence of the HCV polyprotein, leading to the production of the hyperphosphorylated p58 species that is otherwise absent. NS5A may alter c-Raf1-mediated signal transduction only if expressed in the polyprotein context. Therefore, HCV replicon cells HuH-7 I_{377}/NS3-3`/wt/9-13 were compared to naïve HuH-7 cells in the same experimental design. Again, expression of *Renilla reniformis* luciferase (driven by the HSV-TK promoter) was used as an internal standard.

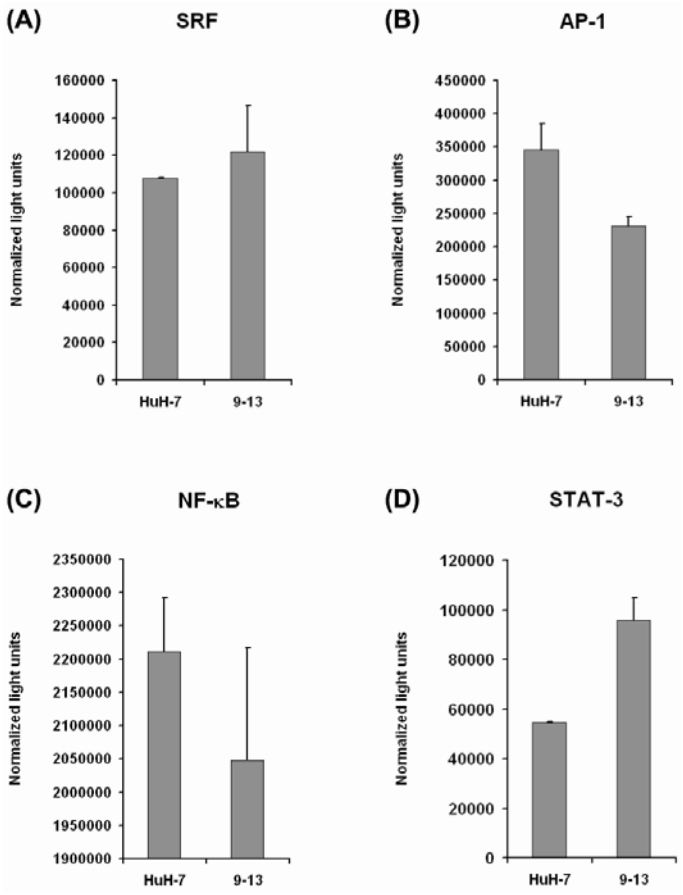

Fig. 5.25 Transcriptional activation of SRF, AP-1, NF-κB or STAT-3 is not altered in HCV replicon cells. HuH-7 cells or HCV replicon cells HuH-7 I_{377}/NS3-3`/wt/9-13 were transfected with 0.3µg of pSRE-Luc (A), pAP-1-Luc (B), pNF-κB-Luc (C) or pSTAT3-TA-Luc (D) as indicated. 0.3µg of pRL-TK was cotransfected with all samples and served as an internal reference. Cells were harvested 48h post transfection and analyzed by measuring both *Photinus pyralis* and *Renilla reniformis* luciferase levels using the Dual-Luciferase Reporter Assay System according to the manufacturer's instructions.

As seen in Fig. 5.25, transcriptional activation from SRF-, AP-1-, NF-κB- or STAT-3-dependent promoters is not altered in HCV replicon cells in comparison to naïve HuH-7 cells either. This confirms the data obtained for NS5A in the absence of the polyprotein context (Fig. 5.23) and indicates that NS5A does not modulate downstream targets of c-Raf1, even if expressed as part of the HCV polyprotein.

Again, NS5A expression was verified by SDS-PAGE and Western blotting using NS5A- or actin-specific antisera.

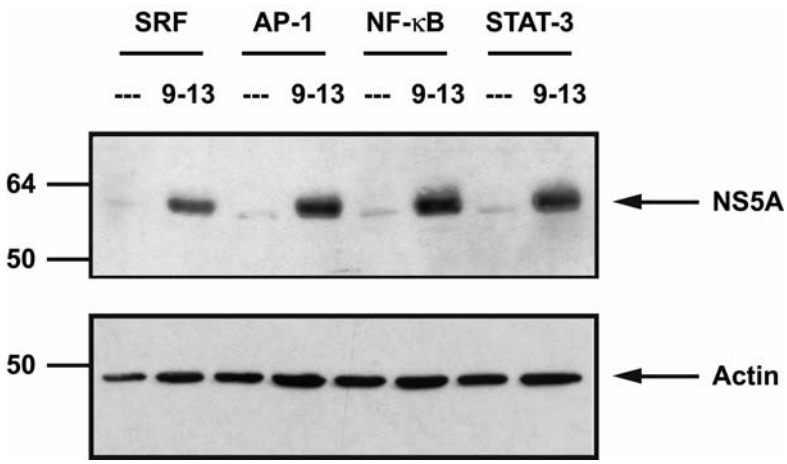

Fig. 5.26 NS5A expression is detected in HCV replicon cells. Naïve HuH-7 cells (---) and HCV replicon cells HuH-7 I_{377}/NS3-3`/wt/9-13 (9-13) were transfected as described in Fig. 5.25. Lysates were subjected to SDS-PAGE and Western blotting using an NS5A-specific antiserum or an actin-specific antiserum (Sigma).

Fig. 5.26 shows that NS5A was properly expressed in the HCV replicon cells that were analyzed in the reporter gene assay (Fig. 5.25). Furthermore, the NS5A double band (p56/p58) is present in these cells, arguing that NS5A was differentially modified in the presence of the polyprotein context.

In summary, these experiments suggest that NS5A does not interfere with c-Raf1-mediated signal transduction. Furthermore, these experiments cast a doubt on previously published data that suggest a role of NS5A in the deregulation of NF-κB and STAT-3.

5.5 Analysis of NS5A phosphorylation.

The experiments described so far demonstrate that c-Raf1 binds to NS5A in several experimental designs. The immunofluorescence analysis (Fig. 5.11) suggests that NS5A binds to the catalytical domain of c-Raf1. Since NS5A is a phosphoprotein and c-Raf1 is a kinase, it was reasonable to hypothesize that NS5A might be a substrate of c-Raf1.

In order to test this hypothesis, NS5A and c-Raf1 were purified by affinity chromatography. Purified proteins were incubated in the presence of [γ-^{32}P] ATP to reconstitute phosphorylation in an *in vitro* assay. Purification of NS5A was described in chapter 5.2.1.

5.5.1 Purification of GST-Raf derived from Sf9 cells.

Expression of c-Raf1 in *E.coli* does not produce any active kinase (W. Kölch, personal communication). This is probably due to misfolding/ aggregation of c-Raf1 in the absence of eukaryotic chaperones. Therefore, in order to obtain purified active c-Raf1, c-Raf1 was expressed in Sf9 cells by infection with a recombinant baculovirus. For convenient purification, c-Raf1 was produced as fusion protein with glutathione S-transferase (GST). As a control, an inactive mutant of c-Raf1 (K375W) was included (Crespo et al., 1994). Both GST-Raf and GST-Raf K375W were purified by glutathione Sepharose chromatography according to the manufacturer's instructions. Purity of the GST-Raf preparations was assessed by silver staining. Identity of the proteins was confirmed by Western blotting using a c-Raf1-specific antiserum.

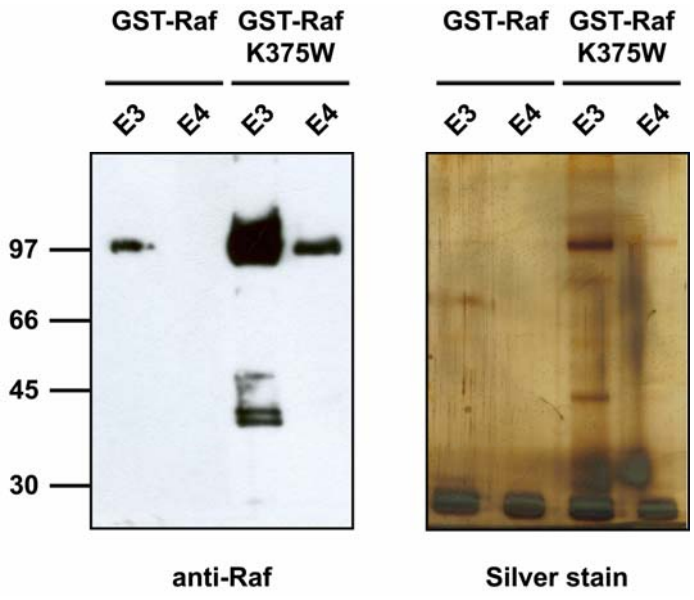

Fig. 5.27 GST-Raf is purified by glutathione Sepharose chromatography. GST-Raf and GST-Raf K375W were expressed in Sf9 cells by infection with recombinant baculoviruses. GST-Raf and GST-Raf K375W were purified by glutathione Sepharose chromatography. Eluate fractions E3 and E4 were analyzed by Western blotting using a c-Raf1-specific antiserum (Santa Cruz) or by silver staining.

As seen in Fig. 5.27, both GST-Raf and GST-Raf K375W were purified by glutathione Sepharose chromatography. However, the yield for GST-Raf was significantly lower than for the inactive mutant GST-Raf K375W. Furthermore, both preparations contained large amounts of an unknown protein migrating below 30kDa. This presumably represents GST that is either endogenously present in Sf9 cells or a degradation product of GST-Raf.
Nevertheless, although the yield was suboptimal for GST-Raf, GST-Raf and GST-Raf K375W were obtained at high purity.

5.5.2 Purified GST-Raf is active whereas GST-Raf K375W is not.

In order to assay whether purified GST-Raf derived from Sf9 cells was active, it was incubated with its endogenous substrate MEK in the presence of [γ-^{32}P] ATP. Since GST-Raf and GST-Raf K375W were not equally concentrated (compare Fig. 5.27), GST-Raf K375W was diluted. Equivalent amounts of GST-Raf and diluted GST-Raf K375W were loaded on an SDS-PAGE and analyzed by Western blotting using a c-Raf1-specific antiserum.

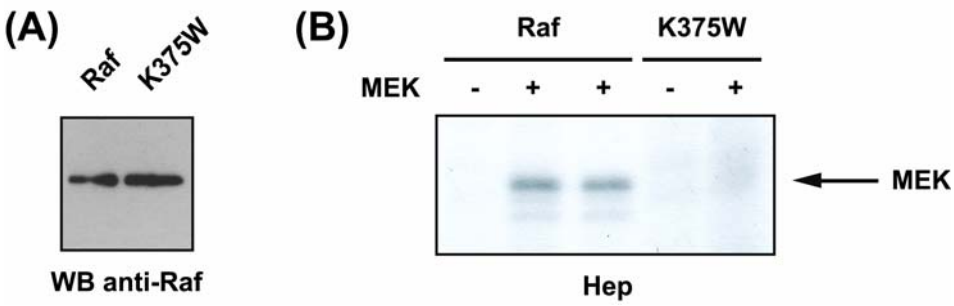

Fig. 5.28 Purified GST-Raf phosphorylates MEK. (A) Purified GST-Raf and GST-Raf K375W were analyzed by Western blotting using a c-Raf1-specific antiserum (Santa Cruz). (B) Purified GST-Raf (and GST-Raf K375W respectively) were incubated with MEK in the presence of [γ-^{32}P]ATP. Samples were electrophoresed on an SDS-PAGE and subjected to autoradiography.

As seen in Fig. 5.28A, GST-Raf and GST-Raf K375W were equally concentrated after dilution of GST-Raf K375W. This was the prerequisite for the *in vitro* phosphorylation assay shown in Fig. 5.28B. The phosphorylation assay indicates that GST-Raf phosphorylates MEK whereas GST-Raf K375W does not. Furthermore, no autophosphorylation of MEK was observed. This suggests that phosphorylation of MEK by c-Raf1 was successfully reconstituted *in vitro*.

5.5.3 GST-Raf is contaminated with kinases that phosphorylate NS5A.

Since GST-Raf was capable of phosphorylating MEK *in vitro*, GST-Raf was incubated with NS5A to see whether GST-Raf was capable of phosphorylating NS5A as well. As additional control, casein kinase II was included because casein kinase II has been shown to phosphorylate NS5A *in vitro* (Kim et al., 1999).

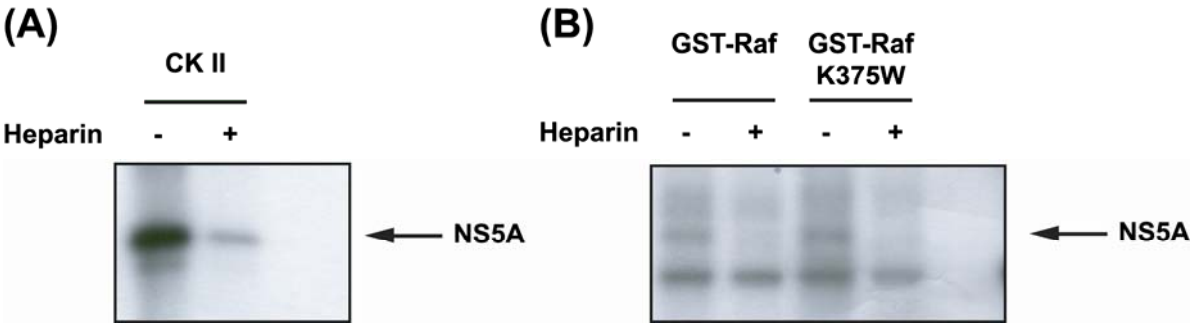

Fig. 5.29 NS5A is phosphorylated by GST-Raf and GST-Raf K375W. (A) Purified casein kinase II was incubated with purified Strep-NS5A-V5 in the presence of [γ-^{32}P]ATP. 400ng/ml of heparin was added as indicated. (B) Purified GST-Raf (and GST-Raf K375W respectively) were incubated with Strep-NS5A-V5 in the presence of [γ-^{32}P]ATP. 400ng/ml of heparin was added as indicated. Samples were electrophoresed on an SDS-PAGE and subjected to autoradiography.

Fig. 5.29A shows that NS5A is phosphorylated by casein kinase II, indicating that the NS5A preparation was suitable for an *in vitro* phosphorylation assay. Moreover, phosphorylation of NS5A was effectively inhibited by addition of heparin which is an established inhibitor of casein kinase II (Janosch et al., 1996). In the absence of kinases, NS5A was not phosphorylated, indicating that NS5A does not possess any autophosphorylating activity. With GST-Raf being active (Fig. 5.28) and NS5A being suitable as a kinase substrate (Fig. 5.29A), the prerequisites were fulfilled to investigate whether NS5A is phosphorylated by GST-Raf *in vitro*.

Fig. 5.29B shows that GST-Raf was indeed capable of phosphorylating NS5A *in vitro*. However, the inactive mutant GST-Raf K375W phosphorylated NS5A to the same extent. This indicates that phosphorylation of NS5A was not specific on behalf of c-Raf1 in this experimental setting. Since, again, NS5A itself was not phosphorylated in the absence of GST-Raf/ GST-Raf K375W, NS5A had to be phosphorylated by kinases associated with GST-Raf.

Casein kinase II is one of the kinases that is frequently found to be associated with c-Raf1 (Janosch et al., 1996). An association of c-Raf1 with casein kinase II would be detrimental in this assay since casein kinase II phosphorylates NS5A *in vitro*. To analyze whether casein kinase II may be the associated kinase responsible for phosphorylation of NS5A in this assay, we added heparin to the phosphorylation reaction. Fig. 5.29 shows that phosphorylation of NS5A by GST-Raf/ GST-Raf K375W was effectively inhibited by heparin. At the same time, heparin did not

inhibit phosphorylation of MEK by c-Raf1 (Fig. 5.28). This suggests that casein kinase II may be the contaminating kinase that phosphorylates NS5A *in vitro*.

5.5.4 GST-Raf purified under highly stringent conditions specifically phosphorylates NS5A.

To get rid of the contaminating kinases that spoiled the GST-Raf preparation, the purification protocol for GST-Raf was modified by an additional washing step with RIPA buffer as previously described (Janosch et al., 1996). Surprisingly, the yields of GST-Raf and GST-Raf K375W were similar, indicating that the additional washing step did not disrupt GST-Raf binding to the glutathione Sepharose material (data not shown). Activity of the highly purified GST-Raf was determined as described in chapter 5.5.2 (data not shown). Highly purified GST-Raf was then incubated with purified NS5A to see whether phosphorylation was affected by the purification protocol.

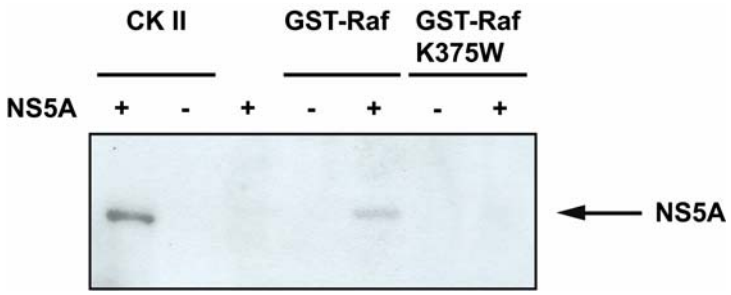

Fig. 5.30 NS5A is specifically phosphorylated by highly purified GST-Raf. Purified casein kinase II or highly purified GST-Raf (and GST-Raf K375W respectively) were incubated with purified Strep-NS5A-V5 in the presence of [γ-^{32}P]ATP. Samples were electrophoresed on an SDS-PAGE and subjected to autoradiography.

Fig. 5.30 shows that NS5A is phosphorylated by highly purified GST-Raf. Phosphorylation is specific for GST-Raf since NS5A is not phosphorylated by GST-Raf K375W or in the absence of exogenous kinase. Phosphorylation of NS5A by GST-Raf was no longer sensitive to heparin (data not shown), indicating that the contaminating kinase that was heparin-sensitive (Fig. 5.29) was no longer present. Again, casein kinase II served as a positive control.

In summary, this experiment demonstrates that NS5A is a substrate of c-Raf1 *in vitro*. Importantly, phosphorylation of GST-Raf is specific and is not caused by kinases associated with GST-Raf.

5.5.5 Inhibition of c-Raf1 leads to a loss of NS5A hyperphosphorylation *in vivo.*

NS5A phosphorylation is classified as either "hypophosphorylation" or "hyperphosphorylation". As mentioned in chapter 1.8, hyperphosphorylation is a very complex phenomenon that is still poorly understood: If NS5A is expressed in the absence of the HCV polyprotein, it migrates as a single band of 56kD in an SDS-PAGE. However, if it is expressed in the context of the HCV polyprotein, an additional band of 58kD appears. Several lines of evidence suggest that this species is a differentially phosphorylated form of NS5A.

The *in vitro* phosphorylation assay suggested that NS5A is a substrate of c-Raf1. If c-Raf1 phosphorylates NS5A *in vivo*, an inhibition of c-Raf1 may affect the distribution between hypophosphorylated p56 and hyperphosphorylated p58. To analyze the impact of c-Raf1-inhibition on NS5A hyperphosphorylation, the HCV replicon cell line HuH-7 I_{377}/NS3-3`/wt/9-13 was used. This is one of the few replicon cell lines that has retained the hyperphosphorylated species. c-Raf1 was inhibited by the means of the small-molecule inhibitor BAY43-9006. BAY43-9006 was applied at different concentrations corresponding to its profile of action (compare Fig. 5.15).

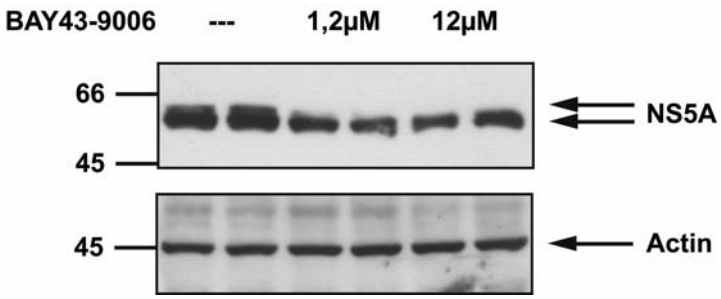

Fig. 5.31 Inhibition of c-Raf1 leads to a loss of NS5A hyperphosphorylation. HCV replicon cells HuH-7 I_{377}/NS3-3`/wt/9-13 were incubated with increasing concentrations of BAY43-9006 for 16h. Cells were harvested and analyzed by Western blotting using an NS5A-specific antiserum.

Incubation of HCV replicon cells with BAY43-9006 lead to a dose-dependent reduction of the hyperphosphorylated species p58 (Fig. 5.31). At the same time, integrity of the cell was unaffected as shown by the actin-specific Western blot. This suggests that integrity of c-Raf1 is a prerequisite for NS5A hyperphosphorylation.

5.6 *Generation and analysis of NS5A-transgenic mice*

5.6.1 Generation of transgenic mice

Chronic HCV infection is frequently associated with liver cirrhosis and hepatocellular carcinoma. However, the mechanism of hepatocarcinogenesis is poorly understood. This is essentially due to the fact that appropriate model systems are not available. In order to analyze the contribution of NS5A to the development of hepatocellular carcinoma, a new model system was established by generating NS5A-transgenic mice that express NS5A in a liver-specific manner.

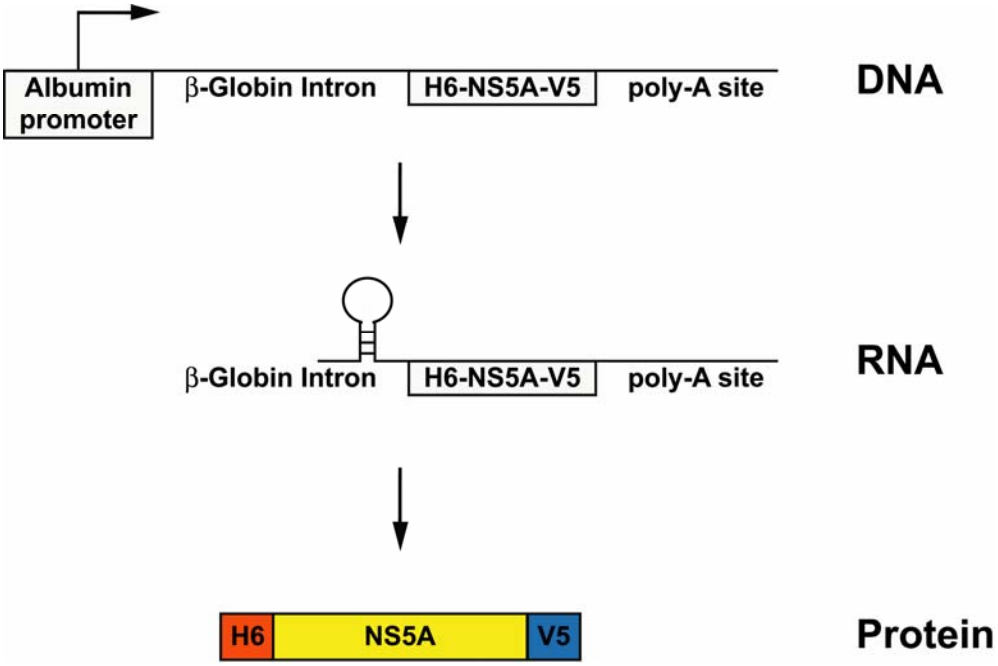

Fig. 5.32 Schematic representation of NS5A expression. NS5A expression is driven by the albumin promoter. The β-globin intron was included to increase transcriptional efficiency. NS5A was expressed as a fusion protein with an N-terminal hexa-histidine tag (H6) and a C-terminal V5-epitope.

To that end, an NS5A expression cassette was subcloned (Fig. 5.32). Expression of NS5A was driven by the minimal albumin promoter that has previously been shown to elicit robust transgene expression in the liver (Chisari et al., 1989). Expression was enhanced by introduction of the β-Globin intron immediately upstream of NS5A. Introduction of introns significantly increases transcriptional efficiency in transgenic mice although the underlying mechanism is unclear (Brinster et al., 1988). NS5A itself was expressed as fusion protein with an N-terminal

hexa-histidine tag and a C-terminal V5 epitope. The V5 epitope was included for convenient detection of NS5A. The hexa-histidine tag allows the enrichment of NS5A by metal chelating chromatography (Ni^{2+}).

The plasmid that contained the expression cassette was digested with restriction endonucleases Not I and Xho I and electrophoresed on an agarose gel (data not shown). The fragment that contained the NS5A expression cassette was purified and microinjected into FVB embryos. The transgenic embryos were implanted into pseudopregnant FVB mice and the offspring was analyzed for presence of the transgene by PCR.

To that end, DNA was extracted from mouse tail biopsies. The DNA was analyzed by duplex-PCR, assaying for both the presence of NS5A and tubulin at the same time. The tubulin-PCR served as an internal reference to indicate whether the DNA preparation was successful or not. A representative result is shown in Fig. 5.33.

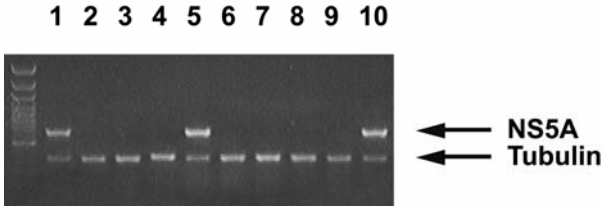

Fig. 5.33 NS5A can be detected in tail biopsies by PCR. DNA was extracted from mouse tail biopsies (mice 1-10) and analyzed by duplex-PCR using both NS5A- and tubulin-specific primers at the same time.

The tubulin-specific PCR indicates that the DNA preparation was successful in all cases. The NS5A-specific PCR shows that animals 1,5 and 10 were transgenic (+/-) whereas the rest was not (-/-). In summary, this demonstrates that NS5A-transgenic mice were easily identified by PCR.

5.6.2 NS5A is expressed in the liver of transgenic mice.

Having established a genotyping protocol, NS5A expression was assessed by the means of RT-PCR. Therefore, RNA was extracted from livers of transgenic mice and non-transgenic littermates. Integrity of the RNA was analyzed by agarose gel electrophoresis (data not shown). The RNA was digested with DNAse and reverse transcribed using an oligo-dT primer. The

resulting cDNA was analyzed by PCR using NS5A-specific primers. In parallel, integrity of the liver cDNA was assayed by PCR using albumin-specific primers. A representative result is shown in Fig. 5.34.

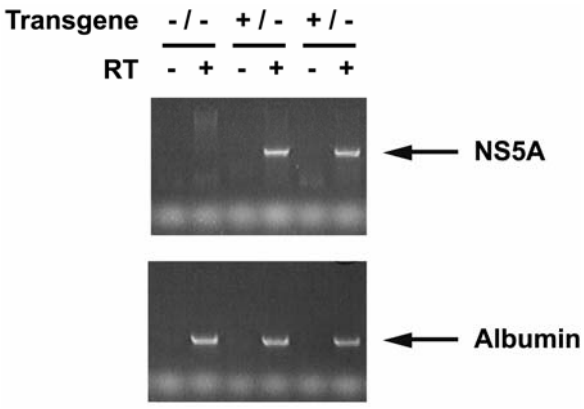

Fig. 5.34 NS5A is expressed in the liver of transgenic mice. RNA was extracted from livers of NS5A-transgenic mice (+/-) and their non-transgenic littermates (-/-). RNA was digested with DNAse and either reverse transcribed (RT +) or not (RT -). The resulting cDNA was analyzed by PCR using NS5A- or albumin-specific primers.

Fig. 5.34 shows that the samples that were not reverse transcribed (RT -) did not produce any PCR product. This demonstrates that the RNA preparation was essentially devoid of genomic DNA. The albumin-specific PCR was positive in all cases, demonstrating that the liver cDNA was intact. The NS5A-specific PCR was only positive for NS5A-transgenic mice (+/-) and not for the non-transgenic littermate (-/-). This indicates that NS5A is expressed in the liver of transgenic mice.

5.6.3 NS5A expression is also detected at the protein level.

Since NS5A expression was readily detected on the RNA level, NS5A expression was also analyzed on the protein level. To that end, the livers of transgenic mice and their non-transgenic littermates were homogenized in denaturing protein sample buffer (Pietschmann et al., 2001). NS5A expression was analyzed by Western blotting using a V5-specific antibody.

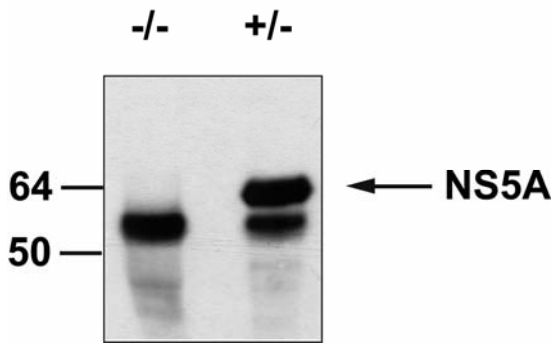

Fig. 5.35 NS5A expression is detected at the protein level. Livers of transgenic mice (+/-) and their non-transgenic littermates (-/-) were lysed in denaturing protein sample buffer and analyzed by Western blotting using a V5-specific antibody (Invitrogen).

Fig. 5.35 shows that expression of the transgene was readily detected in the liver of the transgenic mouse but not in the liver of the non-transgenic littermate. Unfortunately, the NS5A band migrates close to an unspecific band of approximately 55kDa. This band was detected whenever the Western blot was stained with a mouse-derived primary antibody and may therefore represent the IgG heavy chain.

Next, the organ distribution of NS5A was investigated in an NS5A-transgenic mouse. Since NS5A expression is driven by the albumin promoter, NS5A should be detectable in the liver but not in any other organ. To analyze tissue-specificity of NS5A expression, equivalent amounts of liver, kidney, heart, spleen and lung were homogenized in denaturing protein sample buffer. NS5A expression was analyzed by Western blotting using a V5-specific antibody. Since the IgG band mentioned above was not always detectable, ERK2 expression was assayed as a reference.

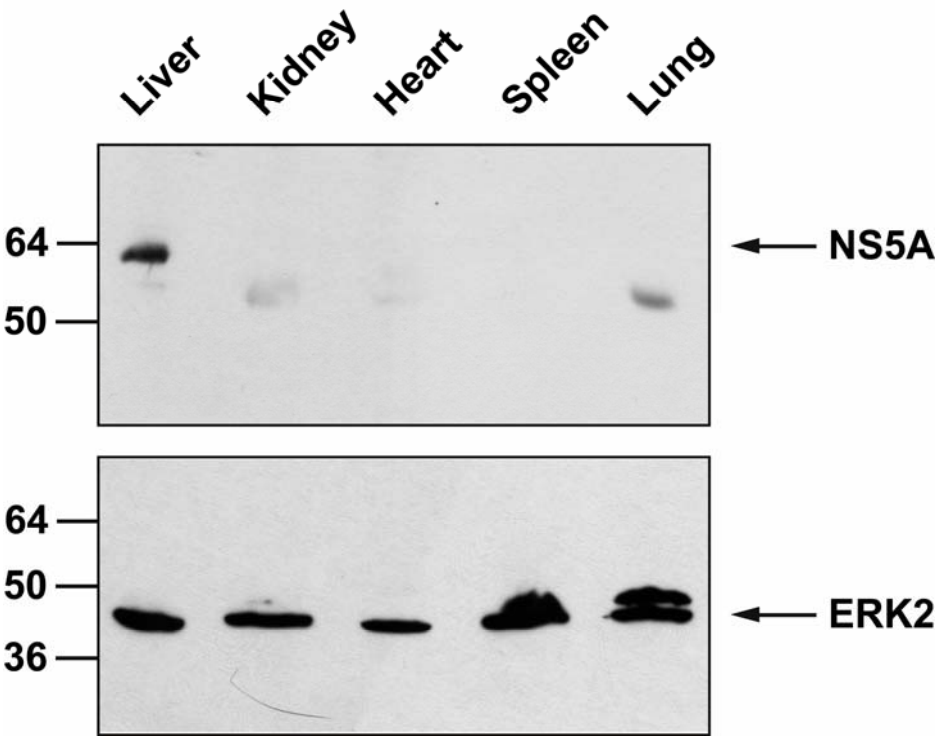

Fig. 5.36 NS5A expression is restricted to liver. Equivalent amounts of liver, kidney, heart, spleen and lung tissue were homogenized in denaturing protein sample buffer and analyzed by Western blotting using either an NS5A- or an ERK2-specific antiserum.

As seen in Fig. 5.36, NS5A is exclusively found in the liver and undetectable in any other organ lysate. At the same time, the ERK2-specific Western blot shows that all lysates contained equivalent amounts of protein. This means that NS5A expression is indeed liver-specific. Expression of NS5A was very stable over time, allowing the detection of NS5A in mice up to nine months of age (latest time point investigated).

These experiments clearly show that NS5A was detected in the livers of transgenic mice. However, it was unknown whether NS5A was homogenously distributed within the liver or whether expression was restricted to a certain region or cell type. Therefore, livers were subjected to cryo-sectioning and cryo-sections were analyzed by the means of immunofluorescence microscopy. To that end, cryo-sections were stained using an NS5A-specific antiserum. As a control, the actin cytoskeleton was stained using FITC-coupled phalloidin.

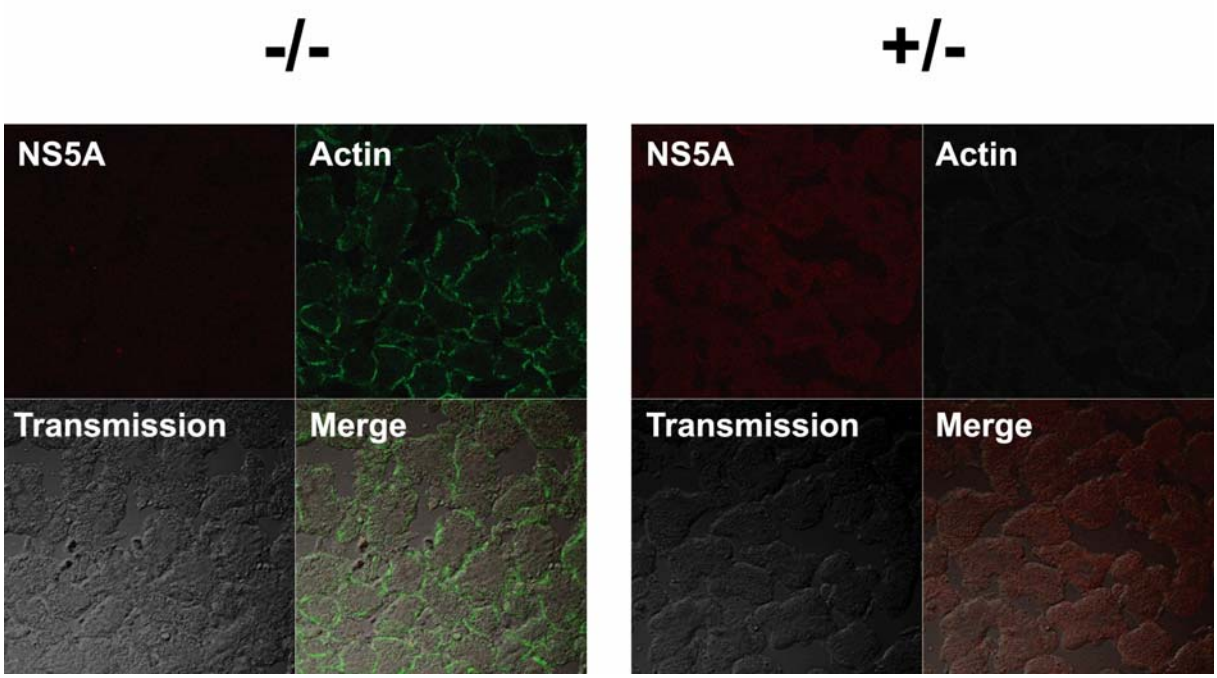

Fig. 5.37 NS5A expression is detected in cryo-sections of transgenic mice. Liver tissue was cryo-sectioned (5µm sections). Cryo-sections were fixed by 4% paraformaldehyde and stained using an NS5A-specific antiserum (Cy3). The actin cytoskeleton was stained using FITC-coupled phalloidin.

The phalloidin staining indicates that the tissue sections are intact (Fig. 5.37). The signal produced by the NS5A-specific antiserum was very weak and diffuse. This indicates that the expression level of NS5A in these sections is rather low. Since the signal is rather diffuse, the subcellular localization of NS5A in these sections could not be investigated. Nevertheless, NS5A could be detected in cryo-sections of transgenic mice.

In summary, the data presented in chapter 5.6.3 document that expression of NS5A is detected at the protein level. Furthermore, liver-specific expression of NS5A was confirmed. Future experiments should focus on the impact of NS5A on HCV-mediated liver pathogenesis.